1-1-2008

Ti-in-zircon thermometry applied to contrasting Archean metamorphic and igneous systems

Joe Hiess
NERC Isotope Geosciences Laboratory

Allen Phillip Nutman
University of Wollongong, anutman@uow.edu.au

Vickie C. Bennett
Australian National University

Peter Holden

Ti-in-zircon thermometry applied to contrasting Archean metamorphic and igneous systems

Abstract

Ti-in-zircon thermometry with SHRIMP II multi-collector has been applied to two well-documented Archean igneous and metamorphic samples from southern West Greenland. Zircons from 2.71 Ga partial melt segregation G03/38 formed in a small (<1>m(3)), closed system within a mafic rock under high pressure granulite facies conditions. Results of 14 Ti analyses present a mean apparent zircon crystallization temperature of 679 +/- 11 degrees C, underestimating independent garnet-clinopyroxene thermometry by 20-50 degrees C but consistent with reduced a(TiO2) in this system. 36 spot analysis on 15 zircons from 3.81 Ga meta-tonalite G97/18, with an estimated magmatic temperature >1000 degrees C, yield a low-temperature focused normal distribution with a mean of 683 +/- 32 degrees C, further demonstrated by high resolution Ti mapping of two individual grains. This distribution is interpreted to represent the temperature of the residual magma at zircon saturation, late in the crystallization history of the tonalite. Hypothetically, Ti-in-zircon thermometry on Eoarchaean detrital zircons sourced from such a high temperature tonalite would present a low-temperature biased image of the host magma, which could be misconstrued as being a minimum melt granite. Multiple analyses from individual zircons can yield complex Ti distributions and associated apparent temperature patterns, reflecting cooling history and local chemical environments in large magma chambers. In addition to inclusions and crystal imperfections, which can yield apparent high temperature anomalies, zircon surfaces can also record extreme (>1000 degrees C) apparent Ti temperatures. In our studies these were traced to (49)Ti (or a molecular isobaric interference) contamination derived from the double sided adhesive tape used in sample preparation, and should not be assigned geological significance. (C) 2007 Elsevier B.V. All rights reserved. Document Type: Article

Keywords

ti, metamorphic, archean, igneous, contrasting, systems, applied, thermometry, zircon, GeoQUEST

Disciplines

Life Sciences | Physical Sciences and Mathematics | Social and Behavioral Sciences

Publication Details

Hiess, J., Nutman, A. Phillip., Bennett, V. C. & Holden, P. (2008). Ti-in-zircon thermometry applied to contrasting Archean metamorphic and igneous systems. Chemical Geology, 247 (3-4), 323-338.

Ti-in-zircon thermometry applied to contrasting Archean metamorphic and igneous systems

Joe Hiess[a]*, Allen P. Nutman[b], Vickie C. Bennett[a], Peter Holden[a]

[a]Research School of Earth Sciences, Australian National University, Canberra, ACT 0200, Australia

[b]Institute of Geology, Chinese Academy of Geological Sciences, 26 Baiwanzhuang Road, Beijing, 100037, China

*Corresponding author.
Research School of Earth Sciences, Building 61, Mills Rd, Australian National University, Canberra, ACT, 0200, Australia.
Phone: +61 2 61255472. Fax: +61 2 61250738. Email: joe.hiess@anu.edu.au

Word count: 261 (abstract)
5592 (text)
973 (references)
621 (captions)

Number of figures: 9
Number of tables: 3
Number of background datasets: 2
(Figures 1, 2, 5, 6 and 9 in black and white for web and print; Figures 3 and 4 in color for web and in black and white for print; Figures 7 and 8 in color for web and print)

Abstract

Ti-in-zircon thermometry with SHRIMP II multi-collector has been applied to two well-documented Archean igneous and metamorphic samples from southern West Greenland. Zircons from 2.71 Ga partial melt segregation G03/38 formed in a small (<1m^3), closed system within a mafic rock under high pressure granulite facies conditions. Results of 14 Ti analyses present a mean apparent zircon crystallization temperature of 679±11°C, underestimating independent garnet-clinopyroxene thermometry by 20-50°C but consistent with reduced a_{TiO2} in this system. 36 spot analysis on 15 zircons from 3.81 Ga meta-tonalite G97/18, with an estimated magmatic temperature >1000°C, yield a low-temperature focused normal distribution with a mean of 683±32°C, further demonstrated by high resolution Ti mapping of two individual grains. This distribution is interpreted to represent the temperature of the residual magma at zircon saturation, late in the crystallization history of the tonalite. Hypothetically, Ti-in-zircon thermometry on Eoarchaean detrital zircons sourced from such a high temperature tonalite would present a low-temperature biased image of the host magma, which could be misconstrued as being a minimum melt granite. Multiple analyses from individual zircons can yield complex Ti distributions and associated apparent temperature patterns, reflecting cooling history and local chemical environments in large magma chambers. In addition to inclusions and crystal imperfections, which can yield apparent high temperature anomalies, zircon surfaces can also record extreme (>1000°C) apparent Ti temperatures. In our studies these were traced to ^{49}Ti (or a molecular isobaric interference) contamination derived from the double sided adhesive tape used in sample preparation, and should not be assigned geological significance.

Keywords: Ti thermometry; zircon; Archean; Greenland; Isua; tonalite

1. Introduction

Incorporation of titanium into crystallizing zircon is seemingly primarily controlled by temperature and a_{TiO2} (Watson et al., 2006), and once within the zircon structure has a very low diffusivity under geologic conditions (Cherniak and Watson, 2007). This thermometer then, has the potential to yield valuable information on the thermal evolution of metamorphic and igneous rocks. Initial application of the Ti-in-zircon thermometer was to 3.91-4.35 Ga detrital zircons from the Jack Hills, Western Australia. The low temperature distributions obtained were used to propose the existence of prograde, wet minimum melting conditions during formation of the granitic protolith to the Hadean zircons (Watson and Harrison, 2005, 2006; Harrison and Schmitt, 2007; Harrison et al. 2007). This hypothesis caries far reaching implications for the dynamics of the early earth and has since stimulated ongoing debate (Nutman, 2006; Valley et al., 2006; Coogan and Hinton, 2006). In order to further explore the validity of applying the experimentally determined Ti-in-zircon thermometer to natural systems, we have examined zircons separated from Archean rocks formed in different conditions. This has the advantage that the chemistry and geologic setting of the host rocks are well known and provides for a more detailed understanding of what Ti signatures from Archean and Hadean detrital zircon populations may reveal about early Earth environments.

The new Ti thermometry results are from zircons from two contrasting Archean samples from southern West Greenland. The first, a 3.81 Ga meta-tonalite represents some of the best preserved Eoarchean felsic crust yet discovered. Such tonalites typically crystallize as large volume magma chambers from melting initiating above 1000°C (Rapp and Watson, 1995). The second sample is from a local, trondhjemitic, minimum melt segregation associated with high pressure granulite facies metamorphism. Each sample has previously determined U/Pb zircon geochronology, petrogenetic constraints and information relevant to the thermal evolution of the rocks (Nutman et al., 1989, 1999; Nutman and Friend, 2007), allowing assessment of under what situations Ti-in-zircon thermometry is best applied.

2. Samples

2.1. 3.81 Ga meta-tonalite sample G97/18

G97/18 is part of the exceptionally well-preserved suite of 3.8 Ga meta-plutonic rocks located between the Isua supracrustal belt and 65°N, initially reported by Nutman et al. (1999). The sample is a homogeneous biotite ± hornblende meta-tonalite with relict igneous texture and very weak biotite foliation (Figure 2 in Nutman et al. (1999)). The trace element characteristics of this sample are typical of Archean tonalite-trondhjemite-granodiorite (TTG) suites, with for example light rare earth element (REE) enrichment, heavy REE depletion, and high Sr/Y. The bulk chemistry of this sample can be modeled by ca. 30% melting of a mafic rock under sufficient pressure to stabilize residual garnet and clinopyroxene (eclogite), with little or no plagioclase fractionation superimposed during emplacement into the crust (Nutman et al., 1999). Extensive experimental data shows that such compositions require temperatures above 1000°C to form (Rapp and Watson, 1995), and thereby would be classified as "hot" granites.

Zircons in the sample are euhedral to subhedral prisms, with generally well-preserved oscillatory igneous zonation. U/Pb geochronology provides a weighted mean $^{207}Pb/^{206}Pb$ age of 3808 ± 4 Ma (n=26, MSWD = 1.9) for oscillatory zoned zircon (Nutman et al., 1999). Crowley (2003) replicated these ages in a U/Pb zircon study using ID-TIMS of tonalites from the same outcrop. There are rare low Th/U replacement domains on the edges of grains as old as 3790 Ma, and some other rare recrystallisation domains have yielded ages as young as 3600 Ma (Nutman et al., 1999). Petrographic studies indicate some zircons contain ilmenite inclusions (Figure 1), which are interpreted to be the predominant Ti-rich phase in equilibrium with the growing igneous zircon. Zircons from this rock, owing to their antiquity, narrow range of ages, and general absence of younger overgrowths have been used in number of geochemical studies including determining the xenon isotopic composition of the Earth at 3.81 Ga. (Honda et al., 2003).

2.2. 2.71 Ga partial melt segregation G03/38

G03/38 collected from Qilanngaarsuit Island, Nuuk district, southern West Greenland was initially reported by Nutman and Friend (2007). The island is dominated by outcrop of the Eoarchaean Itsaq Gneiss Complex (Nutman et al., 1996; Nutman and Friend, 2007) in mylonitic contact with a 2840 Ma tectonic supracrustal slice (Chadwick and Nutman, 1979). On the southern end of the island a ≤200m thick unit of amphibolite and paragneiss preserves small domains of high pressure granulite assemblages. G03/38 is a small (<1m^3), coarse grained, trondhjemitic segregation (Figure 3c. in Nutman and Friend, 2007) in equilibrium with garnet, clinopyroxene and ilmenite from the rock's high pressure granulite assemblage. Mixture modeling using MIX of M (Sambridge and Compston, 1994) on 40 analyses from 29 grains indicated a major zircon age population representing metamorphism at 2714±4 Ma and a minor group representing recrystallisation at 2690±6 Ma (Nutman and Friend, 2007).

Zircons bear rare plagioclase and clinopyroxene inclusions, with only moderate HREE enrichment and negative Eu anomalies, indicating the 2714 Ma zircons should have formed in equilibrium with garnet, clinopyroxene and plagioclase (Nutman and Friend, 2007). The high pressure granulites are commonly partially retrogressed to lower pressure amphibolite facies assemblages, with the replacement of clinopyroxene by hornblendic amphibole and garnet by symplectites containing plagioclase + hornblende. However, locally, such as in sample G03/38, the higher-pressure assemblage is well preserved, with minimal retrogression and many equilibrium boundaries preserved between garnet + clinopyroxene + plagioclase + quartz (Figure 2). This suggests the small trondhjemitic melt segregations developed in the field where dehydration melting of amphibolites starts to occur, at pressures where garnet is stable (Wyllie and Wolf, 1993).

3. Analytical methods

Zircon separates previously extracted from rock samples by conventional crushing, heavy liquid and magnetic techniques were used in this study. Approximately 60 grains from

each sample were transferred onto double sided adhesive tape with a fine-tipped needle under a binocular microscope and flattened onto their c-axis. The grains were shielded with the adhesive tape's paper spacer before being set in epoxy with zircon reference materials SL13 (Claoué-Long et al., 1995), FC1 (Paces and Miller, 1993) and Temora-2 (Black et al., 2003). For the initial analytical session a second mount containing SL13, FC1, Temora-2 zircon reference materials; and NIST 610, 612 and 615 (Pearce et al., 1997) glass reference materials was made. Mounts were polished to expose crystal mid-sections with a rotary polisher and 1μm diamond paste. All grains were imaged with reflected light, transmitted light and cathodoluminesence spectroscopy to identify cracks, inclusions and 2-dimensional growth structure to guide analysis. Prior to each analytical session mounts were sequentially cleaned in an ultrasonic bath with petroleum spirits, ethanol, diluted laboratory detergent, 1M HCl solution, and deionized H_2O before being thoroughly dried in a 60°C oven. A 100Å Au coat was finally applied to the analytical surface and checked to ensure uniform and adequate conductivity before loading into the instrument.

Zircon Ti concentrations were determined using the SHRIMP II multi-collector ion microprobe at the Australian National University over five analytical sessions. Data acquisition and reduction protocols are presented in detail by Aikman (2007) and summarized here. Isotopic ratios were produced by simultaneous measurement of $^{49}Ti^{+}$ with a gain checked, Sjuts continuous dynode electron multiplier at the high mass detector; and $^{28}Si^{16}O^{+}$ by Faraday cup at the low mass detector using count rates $>10^6$ cps. SiO background counts (~0.1% of total SiO counts) were subtracted during setup configuration, ^{49}Ti background counts (2-4 cps) were subtracted during data reduction. Mass resolution was 5,000 at 1% peak height. The low abundance ^{49}Ti isotope (5.41%) was chosen to avoid interference with $^{96}Zr^{2+}$ or $^{48}Ca^{+}$ (from apatite inclusions) on the major ^{48}Ti peak (73.72%) as counting statistics were not a limiting factor for precision.

For spot analysis during the first four analytical sessions a 2.0 to 4.5 nA O_2^- primary beam was focused to a 20μm diameter spot, producing a sensitivity of >19cps ^{49}Ti/ppm Ti/nA O_2^-. Prior to the start of data acquisition a 120μm surface raster was programmed

for 120 seconds to clean the analysis area and avoid Ti contamination from within the gold coat. Data acquisitions consisted of 10-20, 10 second integrations.

Tabulated results from zircon and glass reference materials and the operating conditions specific to each instrument session is presented in Background Dataset 1. $SiO/^{49}Ti$ ratios from zircon and glass reference materials are consistent for concentrations at the ppm level. Internal precision from counting statistics of reference materials is better than 0.2% with external precision matching internal precision during periods of high performance. The standard error from $SiO/^{49}Ti$ ratios on SL13 was <0.7% (n=64) over all five sessions. Temora-2 zircon, FC1 zircon, NIST 610, 612 and 615 glasses were analysed as secondary reference materials to monitor instrument performance, but not directly used to calculate zircon Ti abundances or temperatures.

As part of this study, the Ti concentrations of 23 grains of SL13, FC1 and Temora-2 (previously analysed by SHRIMP) were independently determined by LA-ICPMS. Analysis was performed on the RSES Aligent 7500 ICPMS equipped with a Lamda Physik LPX 1201 UV ArF eximer laser and Ar-He flushed sample cell (Eggins et al., 1998). The laser operated at 22Kv with 100mJ energy per pulse at 5Hz. The 54μm diameter spot was placed directly over the ~1μm deep SHRIMP pits. Each acquisition consisted of a 20 second background followed by a 20 second collection period. Blocks of 10 unknowns were bracketed by analyses of NIST 610 and 612 glass reference material. Raw counts were converted to concentrations using "LABRAT 0.93" written for Lab VIEW by Antti Kallio. Corrections for mass bias drift in unknowns were made using NIST 612. Zircon Ti abundances (Background Dataset 1) were normalized to stoichiometric SiO_2. The mean (2σ) Ti concentration of SL13 was found to be relatively homogeneous (6.3±0.3 ppm, n=10), while Temora-2 (9.1±0.6 ppm, n=6) and FC1 (21.9±1.6 ppm, n=7) are subtly more heterogeneous.

Coinciding SHRIMP ($SiO/^{49}Ti$) and LA-ICPMS [Ti] zircon analyses vary approximately linearly when plotted in $(SiO/^{49}Ti)^{-1}$ vs [Ti] space. This array defines a matrix sensitive regression through the mean value of SL13 and the origin (Figure 3A). This point and

zero calibration line was used to reference the Ti concentration of unknowns from measured $SiO/^{49}Ti$ ratios with well characterized SL13 (Figures 3B and 3C). Ti concentrations for SL13, analysed routinely (typically once every three unknowns during spot analyses) is presented in Figure 3D. This calibration approach is currently limited by reference material heterogeneity and the complex error magnification envelope for unknowns with greater titanium content than the SL13 reference material. Relative errors of <5% are commonly achievable for most geologically useful titanium contents (1-40 ppm).

Command-line software "TiZer" (Aikman, 2007) has been written to process raw SHRIMP multi-collector output files to Ti concentrations and temperatures. $SiO/^{49}Ti$ ratios for single analyses are calculated from scan medians and corrected for drift through the session by robust regression. Ratios are reduced to Ti concentrations using the calibration line described above, and crystallization temperatures using the empirical calibration defined by Watson and Harrison (2005) and Watson et al. (2006). Analytical errors are a product of counting statistics, dispersion in measured $SiO/^{49}Ti$ ratios of reference materials, systematic errors in the Ti content of zircon reference materials (measured by LA-ICPMS) and the uncertainty from the thermometer calibration. Each component of uncertainty is independent. Ti concentration and temperature absolute uncertainties (2σ level) are derived by multiplying uncertainties from each term by their partial derivatives and summing the results in quadrature.

Accurate knowledge of a_{TiO2} and a_{SiO2} at the time of zircon crystallization remains fundamental to the accuracy of the thermometer. Both samples indicate simultaneous crystallization of quartz, zircon and ilmenite suggesting $a_{SiO2} = 1$ and $a_{TiO2} < 1$. All temperatures are uncorrected for $a_{TiO2} < 1$, which in these systems we conservatively estimate to be ~0.6 based on the presence of ilmenite and calculated a_{TiO2} for similar phase assemblages (Ghent and Stout, 1984). This would lead to underestimations of zircon crystallization temperatures by <50°C (Watson and Harrison, 2005).

Following spot analyses, the mount was lightly polished to remove pits from Ti work, then re-cleaned and re-coated with Au for U/Pb geochronology on SHRIMP RG at RSES. The methods used are described in detail by Stern (1998) and Williams (1998) and are summarized here. A 2.5nA primary beam was focused to a 20μm spot diameter and positioned over sites of Ti analysis. A 120μm raster was programmed for 120 sec to clean the mount surface prior to data acquisition. FC1 zircon reference material was analysed once every 3 unknowns. Data reduction was preformed using the Excel^{TM} macro SQUID (Ludwig, 2001). Zircon reference materials SL13 (U = 238 ppm) and FC1 ($^{206}Pb/^{238}U$ age = 1099.0±0.5 Ma) were used for U abundance and $^{206}Pb/^{238}U$ calibrations respectively.

The fifth Ti analytical session involved Ti imaging of selected grains. An ion microprobe is the best tool suited to measure low ppm Ti levels in zircon, with maximum spatial resolution. Imaging allows for determination of the origin of Ti variation as either geologically significant temperature differences, or due to localized features and imperfections such as edge effects, inclusions or cracks in the crystal structure.

Prior to imaging, the mounts were again lightly polished, re-cleaned and re-coated with Au. Zircon grain maps were segmented into blocks to minimize the analytical time spent off the grain and on surrounding epoxy. Each block was setup to run though a matrix with automatic stage drive, primary and secondary tuning. Horizontal and vertical stage movements were programmed to match the spot size so grain coverage was uniform and maximized, without pit overlap or associated geometric effects. Instrumental setup was identical to that described for spot analyses, except a 1.6nA O_2^- primary beam was focused to a ~5μm spot, providing maximum spatial resolution without compromising sensitivity. Prior to the start of data acquisition, a 120 second, 10μm pre-sputter burn-in was programmed directly over the analysis area to clean it of Ti contamination, with minimal disturbance to adjacent analytical sites, or to the sample's potential field defined by the conductive coating. Data acquisitions for each spot consisted of 4, 10 second integrations.

No detectable impact to primary beam focusing or secondary ion yields was observed with progressive removal of the Au layer, or due to the formation of topography on the mount surface from material build-up from adjacent analytical pits. Ti concentrations and temperatures were calculated with TiZer using SL13 zircon reference material analyses separating blocks of unknowns. Concentration values were converted first to 2D matrices and then to unsmoothed Ti intensity grain maps using "Intensity and 3D plot" written for Lab VIEW by Peter Lanc.

New independent temperature estimates for sample G03/38 were determined by WDS mineral analysis on a Camexa SX-51 electron microprobe at the Institute of Geology, the Chinese Academy of Geological Sciences. The vicinity of analysed mineral assemblages was imaged by backscattered electrons (BSE). Garnet-clinopyroxene Fe-Mg exchange thermometry was calculated via the Ellis and Green (1979) calibration using the Excel™ spreadsheet PX-NOM of Sturm (2003).

4. Results

4.1. Spot Analyses

A summary of Ti thermometry and U-Pb dating results for G97/18 and G03/38 spot analyses are presented in Table 1. Composite CL images with analysis locations, crystallization temperatures and $^{207}Pb/^{206}Pb$ ages corrected for very small amounts of common Pb (based on measured ^{204}Pb) are presented in Figures 4 and 5.

4.1.1. G97/18

Zircons from G97/18 are typically ~200µm but upto 300µm in length and prismatic in habit. Oscillatory zonation is fine, running parallel to grain boundaries and locally cut by domains of recrystallization. Fourteen $^{207}Pb/^{206}Pb$ ages range from 3741 to 3833 Ma. Ten analyses on oscillatory zoned zircon indicate ages of >3800 Ma, while three of the four analyses <3800 Ma are recrystallized domains. 36 Ti spot analyses from 15 grains yielded a range of crystallization temperatures from 631°C to 777°C. The normal

distribution is skewed towards its low temperature end, peaking from 660°C to 690°C and with a mean of 683±32°C, 1σ (Figure 6A). Based on growth history identified by oscillatory zonation the dataset consists of 9 grain core analyses (mean = 699±44°C, 1σ), 21 mid grain analyses (mean = 682±25°C, 1σ) and 6 grain edge analyses (mean = 662±19°C, 1σ). Five of the nine core analyses were made on recrystallized areas (mean = 677±33°C, 1σ) but typically show no indication of disturbance to Ti concentrations when compared with adjacent analyses on the same crystal. Six grains received at least three analyses and four grains were analysed twice. From these ten grains with multiple spots, seven show expected systematic trends from apparently high temperature cores that become cooler towards the grain edge; two grains show reverse patterns with lower temperatures towards the grain interior, while one shows an oscillating temperature profile from core to edge. Uncertainties from individual spot temperatures might be broad enough to incorporate at least some of these apparent differences. Rim overgrowth domains were deliberately avoided during these analyses. No systematic relationship exists between Ti temperature and trace element variation as revealed by dark and light CL domains. However, oscillatory zonation in these grains is particularly fine (<5μm), and analysis by the 20μm beam would potentially average micrometer scale compositional variations. Similarly no association can be made between temperature and recrystallised domains, U concentration, Th concentration, U/Th ratio, ^{204}Pb corrected ^{207}Pb/^{206}Pb age or discordance.

4.1.2. G03/38

Zircons from G03/38 are dominantly ~100μm but upto 200μm in length and typically oval to equant in shape. Most display turbid or sector zonation while smaller components are bright and structureless, or show oscillatory zonation. Eleven ^{207}Pb/^{206}Pb ages range from 2666 to 2756 Ma, eight analyses are associated with the recognized 2714±4 Ma peak and three with the minor 2690±6 Ma peak. Fourteen Ti analyses from eleven grains yielded a narrow range of crystallization temperatures from 660°C to 697°C, with a mean of 679°C±11°C, 1σ (Figure 6B). Again no correlation between Ti concentration or temperature and CL, degree of recrystallisation, U, Th, U/Th, ^{204}Pb corrected ^{207}Pb/^{206}Pb or discordance exists.

Results from G03/38 garnet-clinopyroxene mineral analyses are presented in Table 2. Garnet + clinopyroxene + plagioclase + quartz domains display minor alteration by retrogressive reactions, and ilmenite is the main Ti-bearing phase (Figure 2). Within the garnets are well preserved clinopyroxene inclusions, whose edges are unaffected by retrogressive amphibole-forming reactions. Along the edges of garnets are coronas of hornblende + plagioclase, locally as narrow as 100μm. The main garnet + clinopyroxene + plagioclase (An41-42) + quartz assemblage is interpreted to be coeval with the felsic segregation observed in outcrop. This segregation was the source of the zircon used for Ti-in-zircon thermometry.

Garnet-clinopyroxene pairs C and D from the grain interiors (Figure 2) yield temperatures of 700-730ºC (between 6 and 10 kbar). Garnet-clinopyroxene pairs A (at the margin of unaltered clinopyroxene within garnet) and B (separated by a 100 μm hornblende + An45-45 plagioclase corona) give lower temperatures of 590-630ºC (between 6 and 10 kbar).

4.2. Grain Matrix Mapping

Titanium intensity grain maps were produced on grains G97/18-2, G97/18-11 and FC1-7 in order to investigate the details of Ti distribution within single oscillatory zoned grains. Grains from G97/18 were targeted as they emerged with significant Ti variability during spot analyses. FC1-7 was selected to look for an association between large, distinct CL brightness domains and Ti concentrations. The tabulated results are presented in Background Dataset 2.

4.2.1. G97/18-2

Four spot analyses on grain G97/18-2 (Figure 4, Table 1) presented the largest variation of Ti concentration (2.5 to 14.9 ppm) and crystallization temperature (631 to 777°C). The distribution of spot concentrations indicates temperatures are highest at the core and

become lower towards both tips. Hence this grain may provide the best thermal representation of G97/18 zircon growth in the history of one single crystal.

The Ti intensity map for G97/18-2 is presented in Figure 7A with associated reflected light, transmitted light and CL images. The grain appears pristine, free of any cracks or inclusions and to have experienced a smooth, uninhibited growth. Its concentration profile demonstrates a systematic decline in Ti from core to rim with mutually consistent values where spot analyses would overlap. This provides a valuable internal check on the validity of measurements made under different analytical approaches during different sessions. The unsmoothed grain image is constructed of 431 pixels, excluding the 0.0 ppm background. Each pixel represents an independent SHRIMP analysis which yielded concentrations ranging from to 2.0 ppm (617°C) to 572.5 ppm (1289°C). Of these 431 analyses, 59 recorded concentrations >15.0 ppm (16 of these >100.0 ppm) and are irregularly concentrated around the grain's extreme rim. Rim overgrowth domains were avoided during spot analyses, subsequently these high and variable concentrations feature as an unexpected result in the grain matrix map. The figure was constructed with the Ti concentration range capped at 15.0 ppm to highlight the grain's internal variability from core to mid regions rather than extreme concentrations on the grain edge. This limit corresponds to the maximum concentrations measured in the grain's core and represents a crystallization temperature of approximately 778°C.

Ti crystallization temperatures derived from G97/18-2 are presented in Figure 6C. The profile consists of 372 analyses with concentrations from 2.0 ppm (617°C) to 15.0 ppm (778°C). The normal distribution is relatively smooth, uninterrupted, and skewed towards lower temperatures, with a mean of 676±40°C (1σ). Again temperatures associated with rim concentrations >15.0 ppm were filtered from the image. Figure 8 has been added to represent a revised version of the Ti intensity map if >15.0 ppm pixels are excluded. Here the grain appears with a more uniform edge and better resembling morphology from reflected, transmitted and CL imaging.

4.2.2. G97/18-11

Five spot analyses on grain G97/18-11 revealed complex and unsystematic distributions of Ti concentrations (range of 3.5 to 13.6 ppm) and crystallization temperatures (range of 656 to 768°C) that undulate on a transect from the grain core to tip, following oscillatory growth domains identified in CL imaging. Absolute uncertainties on analytical spots provide inadequate overlap to explain these differences.

The Ti intensity map for G97/18-11 is presented in Figure 7B. Orientation has been rotated clockwise ~45° with respect to the grain as presented in Figure 4. Reflected and transmitted light imaging reveal an inclusion and cracks that meet the polished surface. CL imaging makes clear the large recrystallised core and small opaque inclusion within large oscillatory zoned domains. The image is made of 583 pixels of concentrations ranging from 2.0 ppm (616°C) to 68125.4 ppm (4044°C). Of the 583 analyses, 100 recorded concentrations >15.0 ppm with 25 >100.0 ppm. Ti concentrations are again consistent with values from spot analyses where overlapping. The figure concentration range was similarly capped at 15.0 ppm to provide clarity to the image. Highest values are again irregularly distributed around the grain's extreme rim and also penetrate the grain edge with anomalously large excursions occurring near the cracks and inclusion. The distribution of Ti is complex but shows no indication of disturbance in the large recrystallized core that appears as a uniform thermo-chemical domain. In the vicinity of the earlier spot analysis transect, Ti concentrations from pristine zircon appear to display a transient oscillation between approximately 3.0–8.0 ppm.

Crystallization temperatures from G97/18-11 are presented in Figure 6D from 483 analyses of concentrations ranging from 2.0 ppm (616°C) to 14.6 ppm (775°C). The distribution is normal with a locus at the mean of 691±26°C (1σ). Temperatures associated with concentrations >15.0 ppm were again removed from the profile.

4.2.3. FC1-7

No spot analysis was previously performed on grain FC1-7. It was analysed to firstly look for relationship between Ti distribution and spatially resolvable CL domains, and secondly to test if high Ti rims were a unique feature to grains from sample G97/18. The

Ti intensity map for FC1-7 is presented in Figure 7C. The crystal appears pristine, free of any cracks or inclusions. Its concentration profile demonstrates a gradient in Ti from one side to the other but can not be clearly associated with the tone of CL domains. The image comprises 156 pixels with concentrations ranging from 7.9 ppm to 240.7 ppm. 19 analyses recorded concentrations >15.0 ppm, with 11 >100.0 ppm. The highest Ti concentrations are irregularly distributed along the length of the higher concentration side of the crystal. The figure concentration range was capped at 50.0 ppm for clarity.

4.3. Origin of high Ti rims

To further pursue the origin of the very high Ti rims observed on G97/18-2, G97/18-11 and FC1-7, whole zircons from G97/18, G03/38, SL13, FC1 and Temora-2 were depth profiled using LA-ICPMS. Crystals were placed onto a glass slide with double sided adhesive tape and flattened onto their c-axis. Grains were again protected from airborne contamination by the adhesive tape's paper spacer when not inside the LA-ICPMS sample cell or being photographed. Analytical methods were identical to those described above for the reference material calibration except that acquisitions consisted of collection periods of upto 360 seconds to try and penetrate the grains entire thickness. Drilling started from the top surface, and generally passed through the entire grain, the bottom surface, adhesive tape and into the glass slide. Results are presented in Table 3. Grains from every aliquot recorded a marked increase in Ti concentrations on most top and bottom surfaces (Figure 9A). Of the 77 surfaces analysed from 51 grains of G97/18, 86% showed anomalously high Ti concentrations, 90% of the 10 surfaces on 5 grains of G03/38 showed excursions, 53% of the 32 surfaces on 15 grains of SL13 showed excursions, 68% of the 53 surfaces on 32 grains of FC1 showed excursions, 85% of the 27 surfaces on 17 grains of Temora-2 showed excursions. Anomalous Ti values could often be detected within the crystal structure during laser drilling but these probably represent analysis of ilmenite inclusions.

SL13 crystals are broken fragments from a larger zircon megacryst. As such their surfaces are modern features. This suggests that the apparent high Ti rims are an artifact of sample processing rather intrinsic features. To test this, further aliquots of the Temora-

2 reference material were variously subjected to either: (1) air abrasion with pyrite crystals to remove the grain exteriors; (2) HF partial dissolution with 1:1 HF-HCl in a sealed teflon beaker for 24 hours on a 120°C hotplate; (3) repeated acetone, or (4) ethanol rinses with an ultrasonic bath followed by decanting. The aim of this exercise was to remove any surface contamination originating from magmatic chemical disequilibrium, minor phases, residues from sample crushing or milling, heavy liquids or other aspect of sample processing that may resulted in high Ti. Results are presented in Table 3. High Ti rims were still widely observed (on 83% to 100% of analysed surfaces) from all treated aliquots suggesting none of these contamination processes are the cause of this effect.

In a last attempt to understand the origin of these signatures direct analysis of the glass slide, epoxy and adhesive tape used to hold the grains was made. While glass and epoxy produced no anomalies, high Ti excursions from the adhesive tape provided identical enrichment profiles to the grain surfaces (Figure 9B), making this contact medium the favored cause for the excursions. It appears ^{49}Ti (or a molecular isobar) can unevenly mix from the adhesive tape into the adjacent epoxy during mount casting, and also be transferred to the grain's top surface by contact with the adhesive tape's paper spacer, which is commonly placed on top of the zircons to protect them at various times during mount preparation. The Ti signature of the tape may be an organic molecule that is unresolved from ^{49}Ti in the SHRIMP even at the ~5000 mass resolution used during analysis. However, it is noted that similar features have been seen on zircon exteriors by other workers when measuring ^{48}Ti (Harrison and Schmitt, 2007). These features have in some cases been attributed to extreme high temperature geologic events (Trail et al., 2006).

5. Discussion

5.1. Temperatures from zircons of metamorphic rock G03/38

The G03/38 Ti-in-zircon temperatures of 679±11°C (1σ) are based on a calibration that assumes rutile as the Ti-buffering phase. Because the main Ti-bearing phase in G03/38 is

ilmenite the calibration may underestimate the calculated G03/38 zircon temperatures by up to 50°C. With this consideration there is a reasonable agreement between the Ellis and Green (1979) garnet-clinopyroxene Fe-Mg exchange thermometer (700-730ºC) and the Ti-in-zircon thermometer for this sample. Garnet-clinopyroxene pairs A and B give lower temperatures (590-630ºC) probably reflecting conditions during superimposed hydration reactions. These results indicate that well equilibrated metamorphic zircon, which forms over a relatively narrow time interval is capable of yielding precise Ti crystallization temperatures that are relatively consistent with established thermometers, although this will require accurate knowledge of a_{TiO2} for the given system. It suggests the method could be a useful tool for determining (possibly multiple) metamorphic conditions in complicated rocks.

5.2. Ti thermometry of 3.81 Ga meta-tonalite G97/18

Magmatic temperatures expected during formation of tonalitic melt compositions have been constrained by extensive experimental data at above 1000°C (Rapp and Watson, 1995), classifying such lithologies as "hot" granites. Sample G97/18 is free of inherited zircon and has a Zr abundance of 121 ppm (Nutman et al., 1999). Using the zirconium saturation in melts relationship of Watson and Harrison (1983) as a guide, G97/18 should become saturated in zircon at ~729°C, hence zircon should crystallize as a late phase from a residual melt at temperatures significantly less than that of the parental liquidus (cf. Nutman, 2006). Modeling has been used to predict the expected distribution of zircon formation as a function of temperature during cooling of a similar intermediate plutonic system (Harrison and Watson, 2006; Figure 3 in Harrison et al. 2007). These calculations predict the distribution would exist as a broad spectrum, with zircon growth declining away from its high temperature end.

The maximum Ti-in-zircon temperatures from G97/18 tonalite (reaching 777±14°C) are notably higher than those expected from zircon saturation thermometry. However the majority of temperatures (mean of 683±32°C, 1σ), reinforced by detailed mapping of grains G97/18-2 (676±40°C) and G97/18-11 (691±26°C) are significantly lower. These

temperatures and distributions are identical, within errors, to those associated with wet, minimum melt, low temperature granites (Watson and Harrison, 2005). The form of these temperature distributions may reflect real gradients for natural zircon formation in similar plutonic systems over protracted retrograde intervals.

The dataset is not biased by lack of high temperature analyses from any specific crystal domains (such as cores) as we have analyzed entire grain mid-sections. Given a plausible a_{TiO2} for this igneous system of ~0.6, corrections for subunity a_{TiO2} would lead to upward temperature adjustments of <50°C, however, the a_{TiO2} of individual detrital zircons can not be precisely known. Subsequently, analysis of Eoarchaean detrital zircons derived from a tonalite such as G97/18 would present a low temperature biased image for their magma source and perhaps lead to the erroneous interpretation of their origin in a minimum melt, low temperature granite.

In some grains the distribution of Ti can be correlated to core and rim domains identified by grain imaging. Trends of Ti variation are consistent with processes of magma cooling (such as in grain G97/18-2) and less frequently as magma recharge or grain convection (in grain G97/18-11). However, during a recharge scenario the introduction of hot, Zr undersaturated melt in the presence of late-crystallizing zircons would be likely to partially or entirely dissolve existing grains (Watson, 1996; Nutman et al., 1999; Mojzsis and Harrison, 2002). No indication of dissolution is found on any crystal. Hence a favored alternative interpretation to the oscillating Ti variations seen in G97/18-11 relates to local disequilibrium in trace element partitioning at the zircon/melt interface (Hoskin, 2000).

6. Conclusions

The Ti-in-zircon thermometer can provide precise temperature estimates in well-equilibrated high grade metamorphic systems. However the accuracy will depend on

accurate knowledge of the a_{TiO2}. Large igneous systems such as those that produce tonalites, undersaturated in Zr and with $a_{TiO2} < 1$, produce low apparent Ti-in-zircon temperatures and distributions that may accurately record the crystallization temperatures of zircon, but likely underestimate that of the parental melt. An inference from this study is that detrital zircons from a rock like tonalite G97/18 would yield low temperature distributions, which could lead to an erroneous interpretation of the lithology from which these zircons were eroded. Thus, there is an inability to distinguish with confidence, using only Ti thermometry, zircons grown in granitic magmas generated by "hot" (900-1000°C) and "cool" (650-750°C) melting. Furthermore individual zircons from large magma chambers can yield complex Ti temperature distributions reflecting variable cooling histories and local chemical environments. Apparent extreme (>1000°C) Ti-in-zircon temperatures derived from zircon rims of samples and reference materials are an artifact of sample preparation. Our study monitoring mass ^{49}Ti has traced the origin of excess Ti to a contaminant in the double sided adhesive tape on which zircons are held prior to casting in epoxy mounts, or on which they are held during laser ablation ICP-MS depth-profiling. Caution in assigning geologic meaning to temperatures from near grain surfaces as well as inclusions and cracks is emphasized.

Acknowledgments

Sample G97/18 was collected during Greenland fieldwork funded by the Research School of Earth Sciences (ANU). In this respect, we wish to thank Prof. David Green. Collection of sample G03/38 and all analytical work was supported by the Australian Research Council grants DP0342798 and DP0342794. Analytical work was undertaken while Hiess was a PhD student at ANU supported by APA and Jaeger scholarships. We thank Shane Paxton and Jon Mya for zircon separations; Chuck McGee for technical assistance with LA-ICPMS analysis; Amos Aikman, Antti Kallio and Peter Lanc for providing software and advice in data processing; Trevor Ireland, Ian Williams, Joerg Herman and Charlotte Allen for helpful discussions. The manuscript was improved by helpful reviews from Laurence Coogan and Paul Hoskin.

584
585
References
587
588 Aikman, A., 2007. Tectonics of the eastern Tethyan Himalaya. Unpublished Ph.D.
589 Thesis, RSES, ANU, Canberra, ACT, Australia.
590
591 Black, L.P., Kamo, S.L., Allen, C.M., Aleinikoff, J.N., Davis, D.W., Korsch, R.J.,
592 Foudoulis, C., 2003. TEMORA 1: a new zircon standard for phanerozoic U–Pb
593 geochronology. Chemical Geology 200, 155–170.
594
595 Chadwick, B., Nutman, A.P., 1979. Archaean structural evolution in the northwest of the
596 Buksefjorden Region, southern West Greenland. Precambrian Research 9, 199-226.
597
598 Cherniak, D.J., Watson, E.B., 2007. Ti Diffusion in zircon. Chemical Geology 242, 470-
599 483.
600
601 Claoué-Long, J.C., Compston, W., Roberts, J., Fanning, C.M., 1995. Two Carboniferous
602 ages: a comparison of SHRIMP zircon dating with conventional zircon ages and
603 $^{40}Ar/^{39}Ar$ analysis. In: Berggren, W.A., Kent, D.V., Aubry, M.P., Hardenbol, J., (Eds.),
604 Geochronology, Time Scales and Global Stratigraphic Correlation. SEPM Special
605 Publication 54, 3-21.
606
607 Coogan, L.A., Hinton, R.W., 2006. Do the trace element compositions of detrital zircons
608 require Hadean continental crust? Geology 34, 633-636.
609
610 Crowley, J.L., 2003. U-Pb geochronology of 3810-3630 Ma granitoid rocks south of the
611 Isua greenstone belt, southern West Greenland. Precambrian Research 126, 235-257.
612

613 Eggins, S., Rudnick, R.L., McDonough, W.F., 1998. The composition of peridotites and
614 their minerals: a laser ablation ICP-MS study. Earth and Planetary Science Letters 154,
615 53-71.
616
617 Ellis, D.J., Green, D.H., 1979. An experimental study of the effects of Ca on garnet-
618 clinopyroxene Fe-Mg exchange equilibria. Contributions to Mineralogy and Petrology
619 71, 13-22.
620
621 Ghent, E.D., Stout, M.Z., 1984. TiO2 activity in metamorphosed pelitic and basic rocks:
622 principles and applications to metamorphism in southeastern Canadian Cordillera.
623 Contributions to Mineralogy and Petrology 86, 248-255.
624
625 Harrison, M., Watson, B., 2006. Interpretation of Ti-in-zircon Thermometery in Plutonic
626 Rocks, Eos Trans. AGU, 87, V31F-03.
627
628 Harrison, T.M., Schmitt, A.K., 2007. High sensitivity mapping of Ti distributions in
629 Hadean zircons. Earth and Planetary Science Letters 261, 9-19.
630
631 Harrison, T.M., Watson, E.B., Aikman, A.B., 2007. Temperature spectra of zircon
632 crystallization in plutonic rocks. Geology 35, 635-638.
633
634 Honda, M., Nutman, A.P., Bennett, V.C., 2003. Xenon compositions of magmatic zircons
635 in 3.64 and 3.81 Ga meta-granitoids from Greenland; a search for extinct ^{244}Pu in ancient
636 terrestrial rocks. Earth and Planetary Science Letters 207, 69-82.
637
638 Hoskin, P.W.O., 2000. Patterns of chaos: Fractal statistics and the oscillatory chemistry
639 of zircon. Geochimica et Cosmochimica Acta 64, 1905-1923.
640
641 Ludwig, K.R., 2001. Squid 1.02 User's Manual, Berkley Geochronology Centre Special
642 Publication No. 2., Rev. June 20. 19p.
643

644 Mojzsis, S.J., Harrison, T.M., 2002. Establishment of a 3.83-Ga magmatic age for the
645 Akilia tonalite (southern West Greenland). Earth and Planetary Science Letters 202, 563-
646 576.
647
648 Nutman, A.P., 2006. Comment on "Zircon Thermometer Reveals Minimum Melting
649 Conditions on Earliest Earth". Science 311, 779b.
650
651 Nutman, A.P., Friend, C.R.L., 2007. Adjacent terranes with ca. 2715 and 2650 Ma high-
652 pressure metamorphic assemblages in the Nuuk region of the North Atlantic Craton,
653 southern West Greenland: Complexities of Neoarchaean collisional orogeny.
654 Precambrian Research 155, 159–203.
655
656 Nutman, A.P., Friend, C.R.L., Baadsgaard, H., McGregor, V.R., 1989. Evolution and
657 assembly of Archean gneiss terranes in the Godthåbsfjord region, southern west
658 Greenland: structural, metamorphic and isotopic evidence. Tectonics 8, 573-589.
659
660 Nutman, A.P., McGregor, V.R., Friend, C.R.L., Bennett, V.C., Kinny, P.D., 1996. The
661 Itsaq gneiss complex of southern West Greenland; the world's most extensive record of
662 early crustal evolution (3900-3600 Ma). Precambrian Research 78, 1-39.
663
664 Nutman, A.P., Bennett, V.C., Friend, C.R.L., Norman, M.D., 1999. Meta-igneous (non-
665 gneissic) tonalites and quartzdiorites from an extensive ca. 3800 Ma terrain south of the
666 Isua supracrustal belt, southern West Greenland; constraints on early crust formation.
667 Contributions to Mineralogy and Petrology 137, 364-388.
668
669 Paces, J.B., Miller, J.D., 1993. Precise U-Pb age of Duluth Complex and related mafic
670 intrusions, northeastern Minnesota: Geochronological insights to physical, petrogenetic,
671 paleomagnetic, and tectonomagnetic processes associated with the 1.1 Ga midcontinent
672 rift system. Journal of Geophysical Research 98, 13997–14013.
673

674 Pearce, N., Perkins, J., Westgate, J., Gorton, M., Jackson, S., Neal, C., Chenery, S., 1997.
675 A compilation of new and published major and trace element data for NIST SRM 610
676 and NIST SRM 612 glass reference materials. Geostandards Newsletter 21, 115-144.
677
678 Rapp, R.P., Watson, E.B., 1995. Dehydration Melting of Metabasalt at
679 8-32 kbar: Implications for Continental Growth and Crust-Mantle Recycling. Journal of
680 Petrology 36, 891-931.
681
682 Sambridge, M.S, Compston, W., 1994. Mixture modelling of multicomponent data sets
683 with application to ion-probe zircon ages. Earth and Planetary Science Letters 128, 373–
684 390.
685
686 Stern, R.A., Bleeker, W., 1998. Age of the world's oldest rocks refined using Canada's
687 SHRIMP: the Acasta Gneiss Complex, Northwest Territories, Canada. Geoscience
688 Canada 25, 27–31.
689
690 Sturm, R., 2003. PX-NOM – an interactive spreadsheet program for the computation of
691 pyroxene analyses derived from the electron microprobe. Computers and Geosciences,
692 28, 473-483.
693
694 Trail, D., Mojzsis, S.J., Harrison, T.M., Levison, H.F., 2006. Do Hadean zircons retain a
695 record of the late heavy bombardment on Earth? Lunar and Planetary Science Conference
696 XXXVII, 2139 Houston, Texas.
697
698 Valley, J.W., Cavosie, A.J., Fu, B., Peck, W.H., Wilde, S.A., 2006. Comment on
699 "Heterogeneous Hadean Hafnium: Evidence of Continental Crust at 4.4 to 4.5 Ga",
700 Science 312, 1139a.
701
702 Watson, E.B., 1996. Dissolution, growth and survival of zircons during crustal fusion;
703 kinetic principles, geological models and implications for isotopic inheritance. Special
704 Paper of the Geological Society of America 315, 43-56.

Watson, E.B., Harrison, T.M., 1983. Zircon saturation revisited: temperature and composition effects in a variety of crustal magma types. Earth and Planetary Science Letters 64, 295-304.

Watson, E.B., Harrison, T.M., 2005. Zircon thermometer reveals minimum melting conditions on earliest Earth. Science 308, 841-844.

Watson, E.B., Harrison, T.M., 2006. Response to Comments on "Zircon Thermometer Reveals Minimum Melting Conditions on Earliest Earth". Science 311, 779c.

Watson, E.B., Wark, D., Thomas, J., 2006. Crystallization thermometers for zircon and rutile. Contributions to Mineralogy and Petrology 151, 413-433.

Williams, I.S., 1998. U-Th-Pb geochronology by ion microprobe. Reviews in Economic Geology 7, 1-35.

Wyllie, P.J., Wolf, M.B., 1993. Amphibolite-dehydration melting: sorting out the solidus. In: Pritchard, H.M., Alabaster, T., Harris, N.B.W., Neary, C.R., (Eds.) Magmatic Processes and Plate Tectonics. Geological Society Special Paper 76, 405-416.

Figure Captions

Figure 1.
Cathodoluminesence (CL) and transmitted light (trans) images of fine oscillatory zoned G97/18 grain with exposed ilmenite (ilm) inclusion.

Figure 2.
Backscattered electron image of G03/38 high pressure assemblage with well preserved garnet (gnt) + clinopyroxene (cpx) + plagioclase (plag) + quartz (qtz) equilibrium

boundaries. Retrogression to hornblende (hbl) is minimal. A, B, C and D indicate locations of garnet and clinopyroxene WDS mineral analysis.

Figure 3.

Zircon calibration and reference material data A) SHRIMP $^{49}Ti/SiO$ vs LA-ICPMS [Ti] linear relationship from SL13, Temora-2 and FC1 reference materials. Point and zero calibration line passes from the origin through the mean of SL13 values; B) SHRIMP $^{49}Ti/SiO$ with TiZer calculated [Ti] for unknowns and related reference materials from sessions 1-4; C) As B) for session 5; D) Summary of Ti concentrations from 64 analyses of SL13 over all sessions. Mean = 6.14±0.02 ppm (2σ).

Figure 4.

Composite CL image for G97/18 sample zircons with analysis spots, uncorrected crystallization temperatures and $^{207}Pb/^{206}Pb$ ages. Grains G97/18-2 and G97/18-11 reveal complex temperature profiles targeted for Ti matrix mapping.

Figure 5.

Composite CL image with analysis spots, uncorrected crystallization temperatures and $^{207}Pb/^{206}Pb$ ages for zircon of sample G03/38. Note the narrow range of crystallization temperatures for this simple closed system.

Figure 6.

Histogram and probability density plots of uncorrected crystallization temperatures for A) spot analysis of sample G97/18, B) spot analysis of sample G03/38, C) mapping of single grain G97/18-2, D) mapping of single grain G97/18-11. Temperatures associated with Ti concentrations >15.0 ppm (>778°C) and >14.6 ppm (>775°C) filtered from figures C and D respectively.

Figure 7.

From left to right: reflected light, transmitted light, CL images and Ti concentration maps for grains A) G97/18-2, length of crystal 200μm, note highest concentrations observed in

Figure 1

Click here to download high resolution image

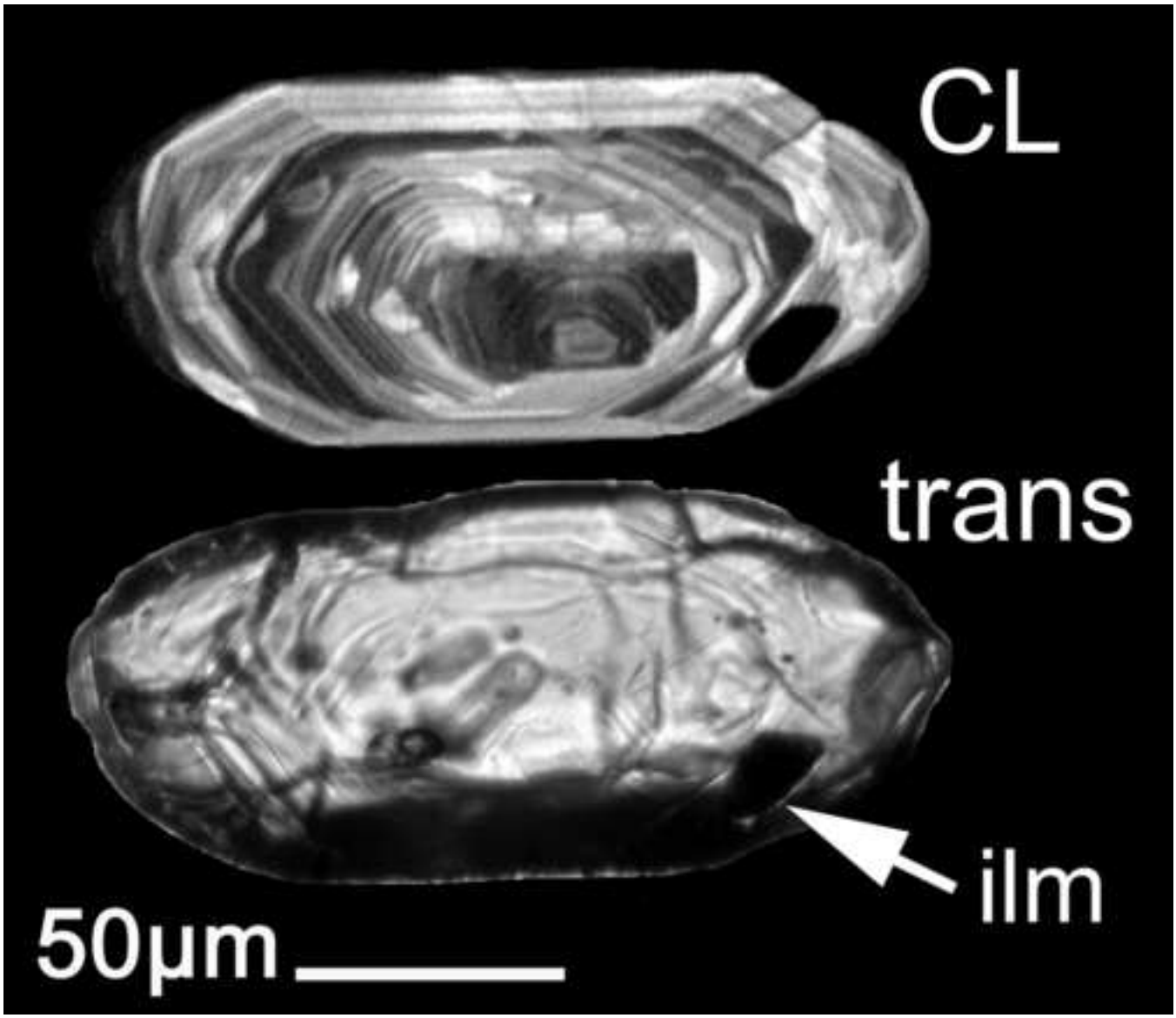

Figure 2

Click here to download high resolution image

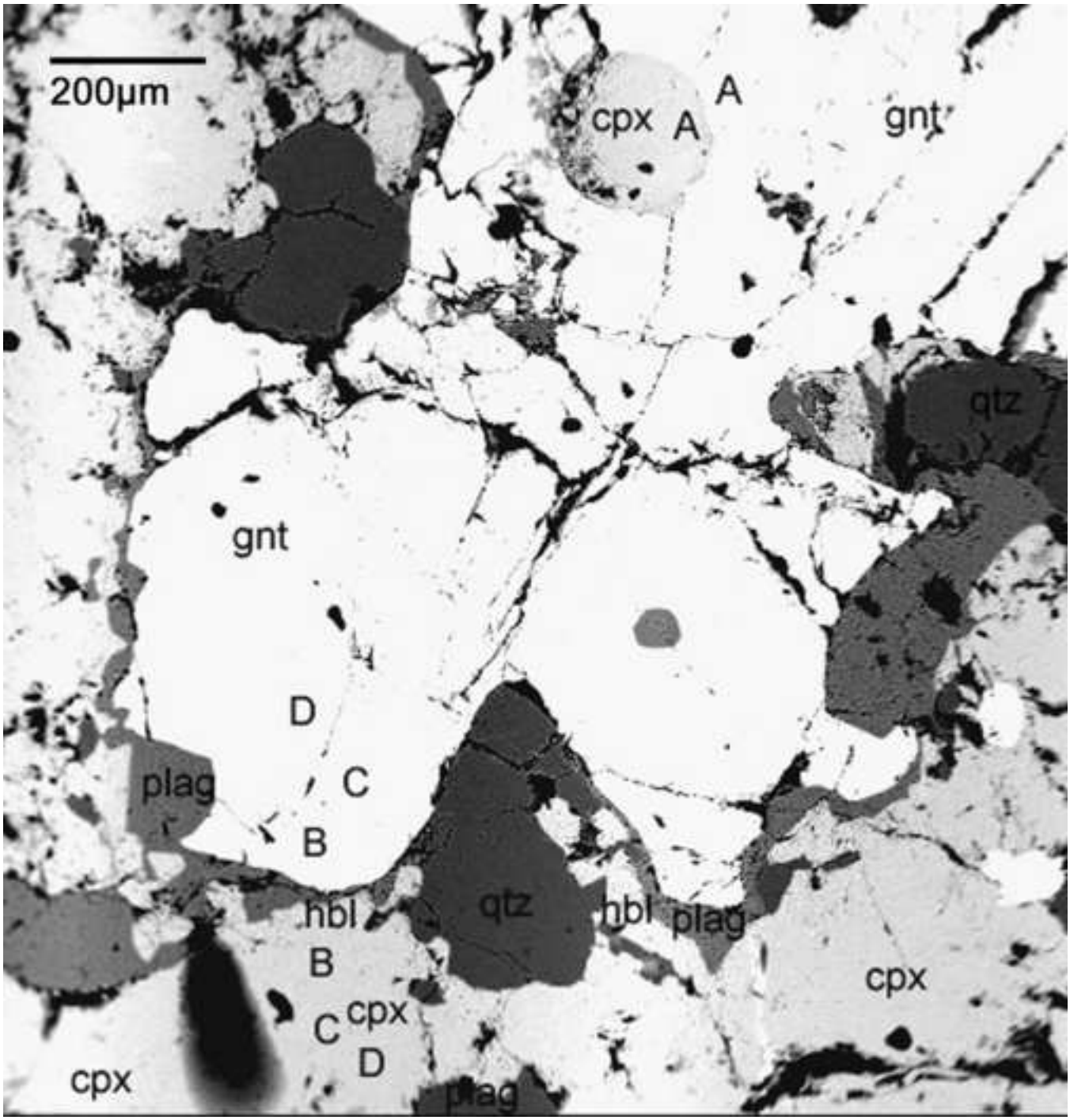

Figure 3

Click here to download high resolution image

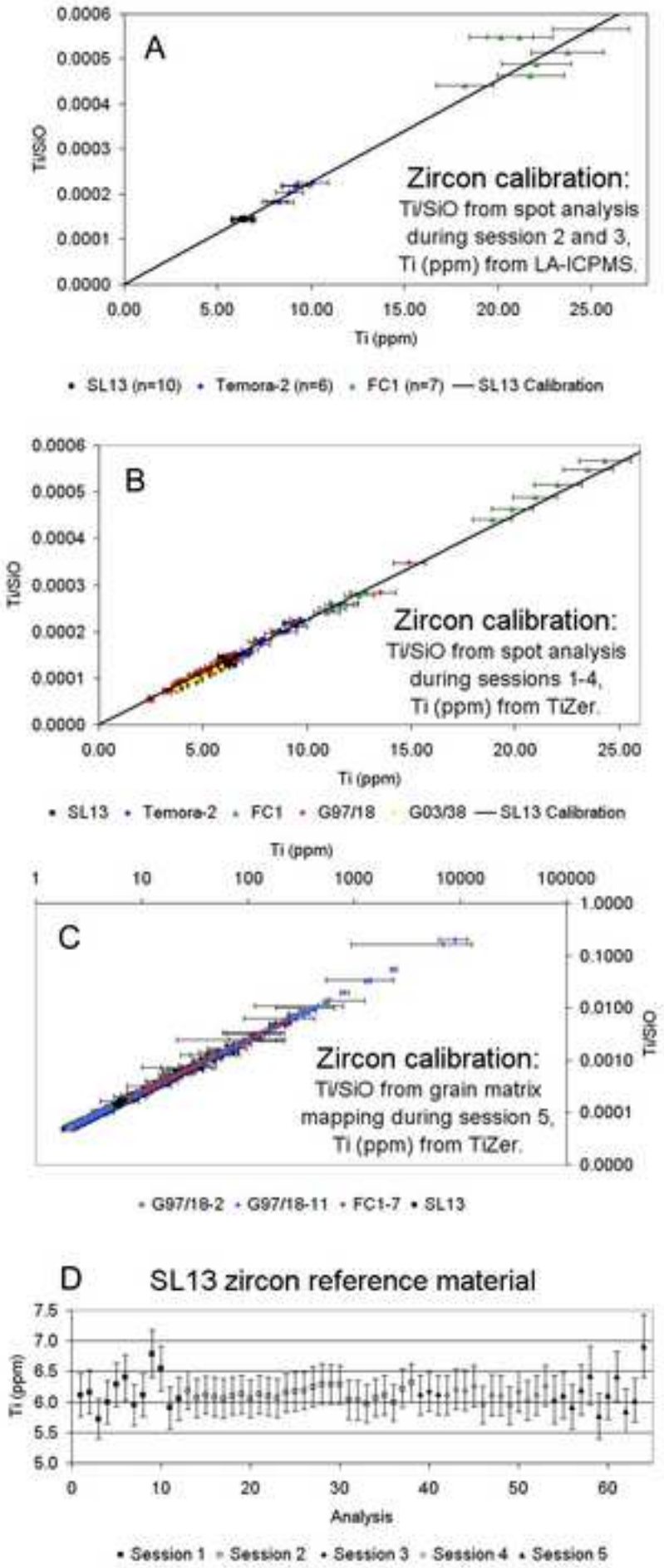

Figure 4

Click here to download high resolution image

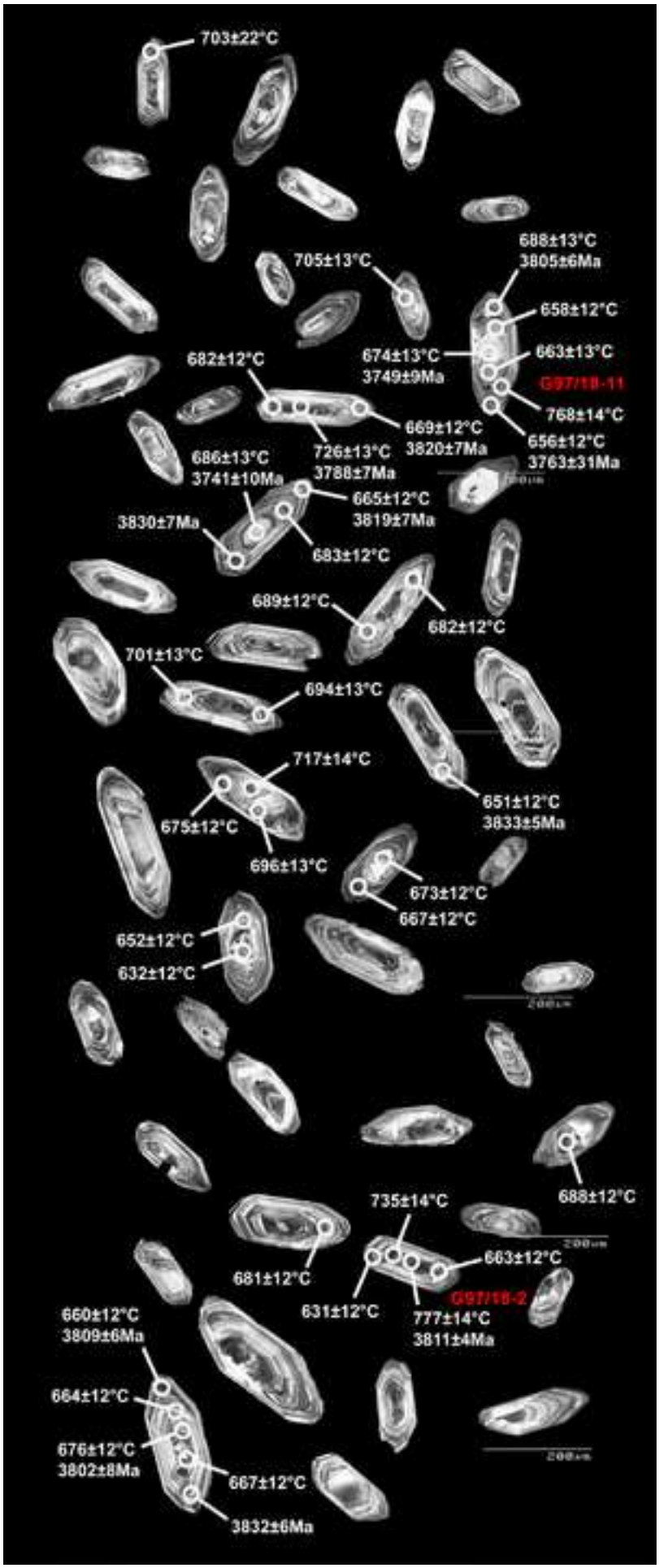

Figure 5

Click here to download high resolution image

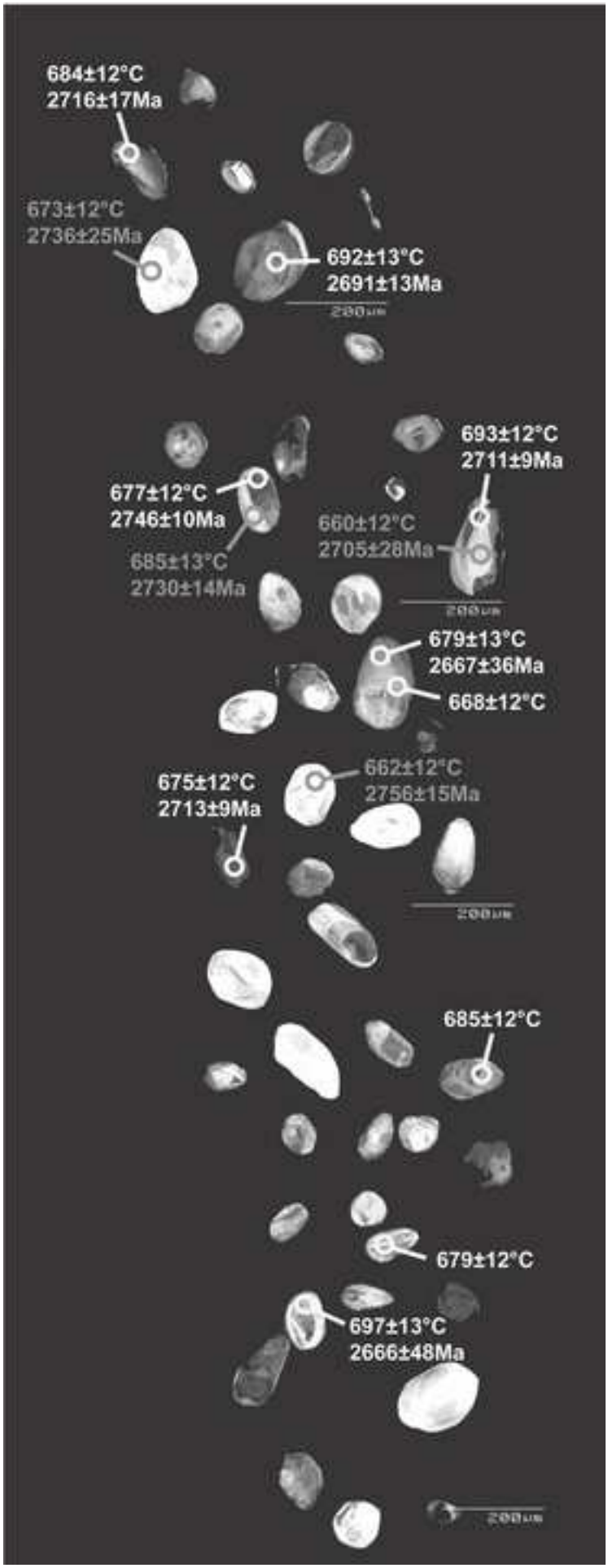

Figure 6

Click here to download high resolution image

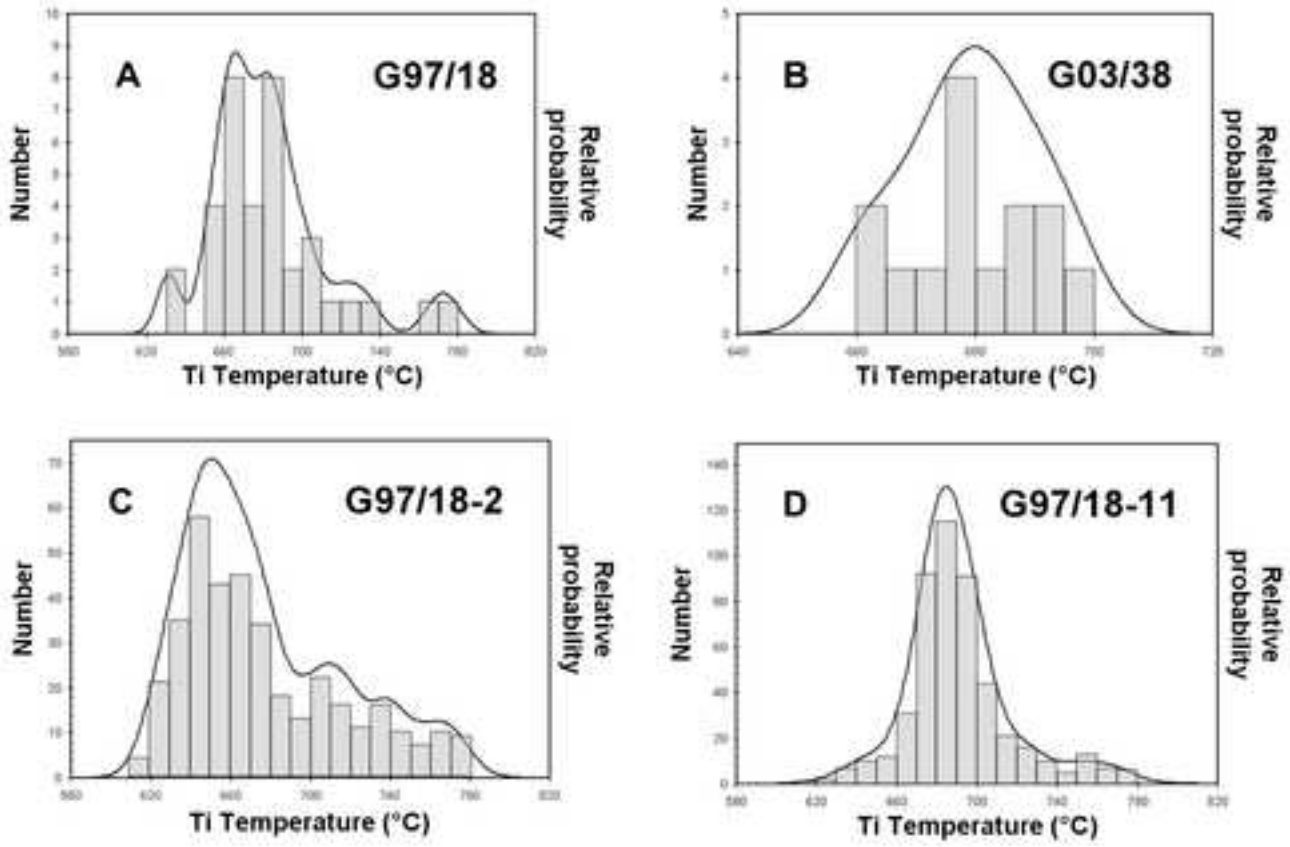

Figure 7

Click here to download high resolution image

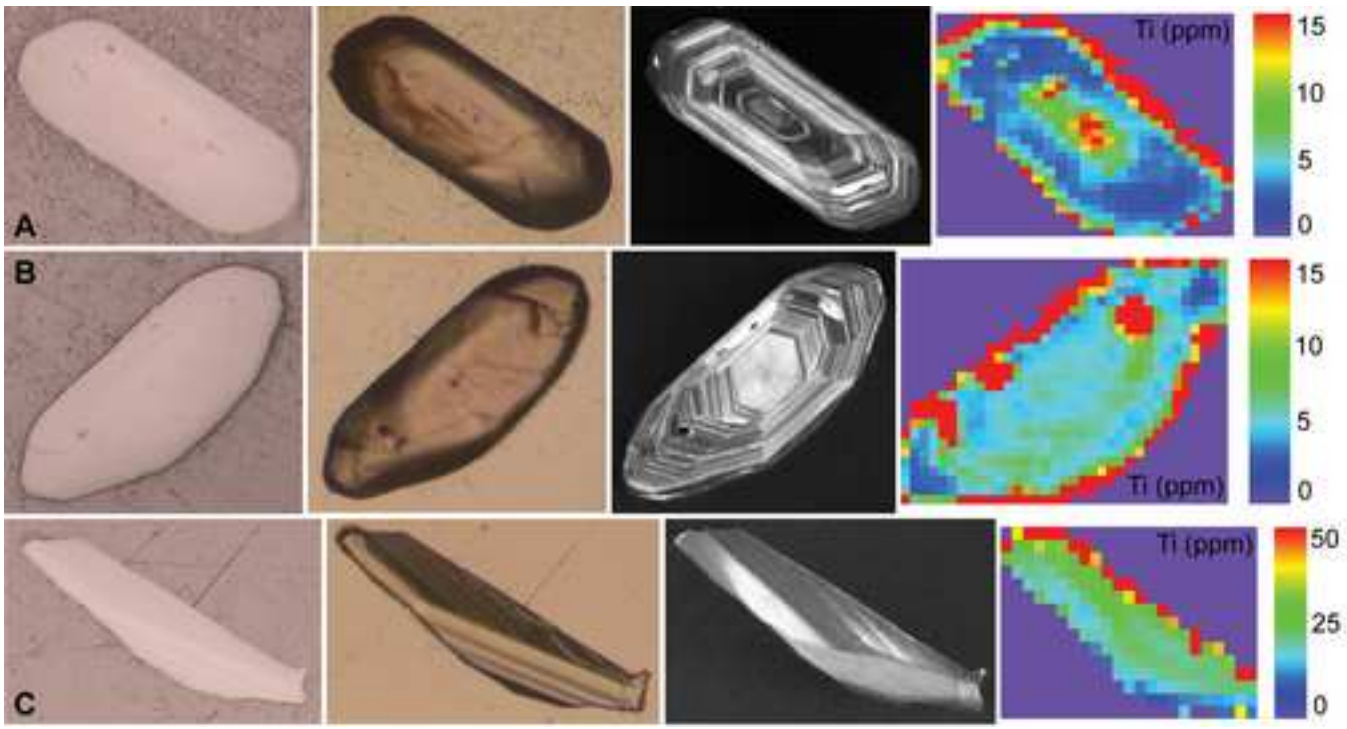

Figure 8

Click here to download high resolution image

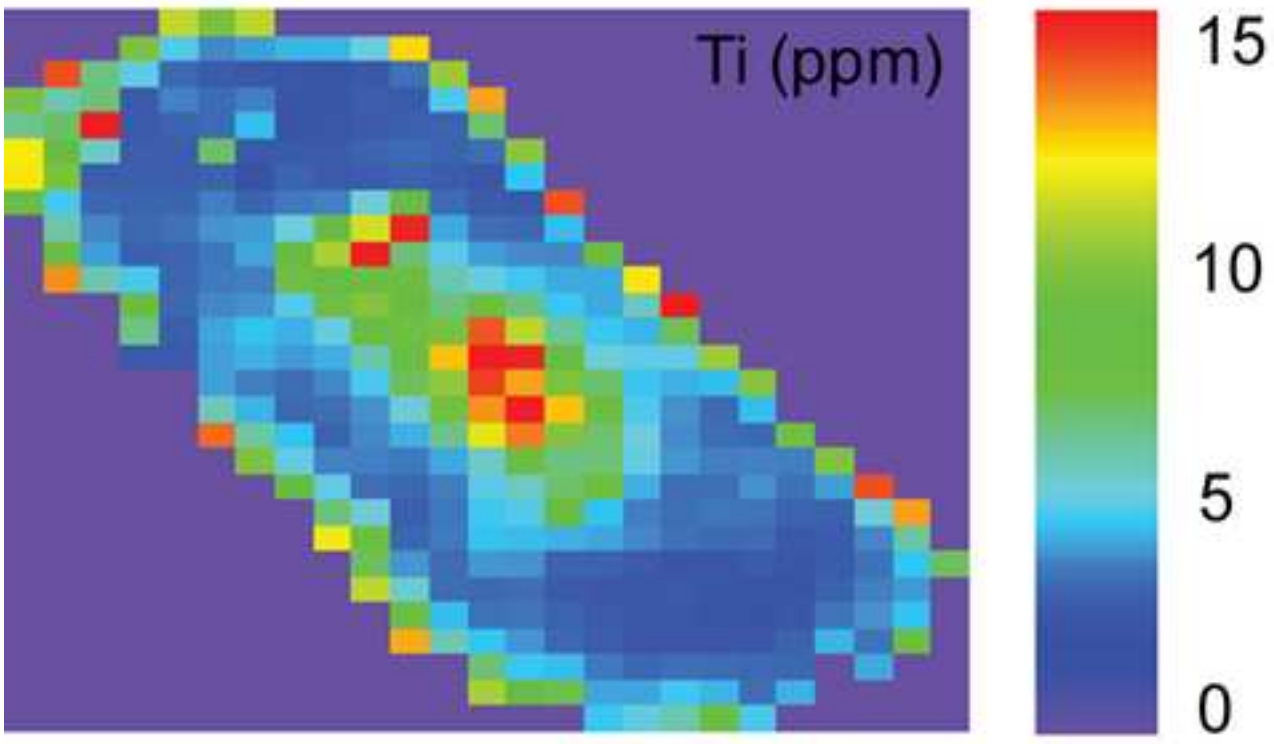

Figure 9

Click here to download high resolution image

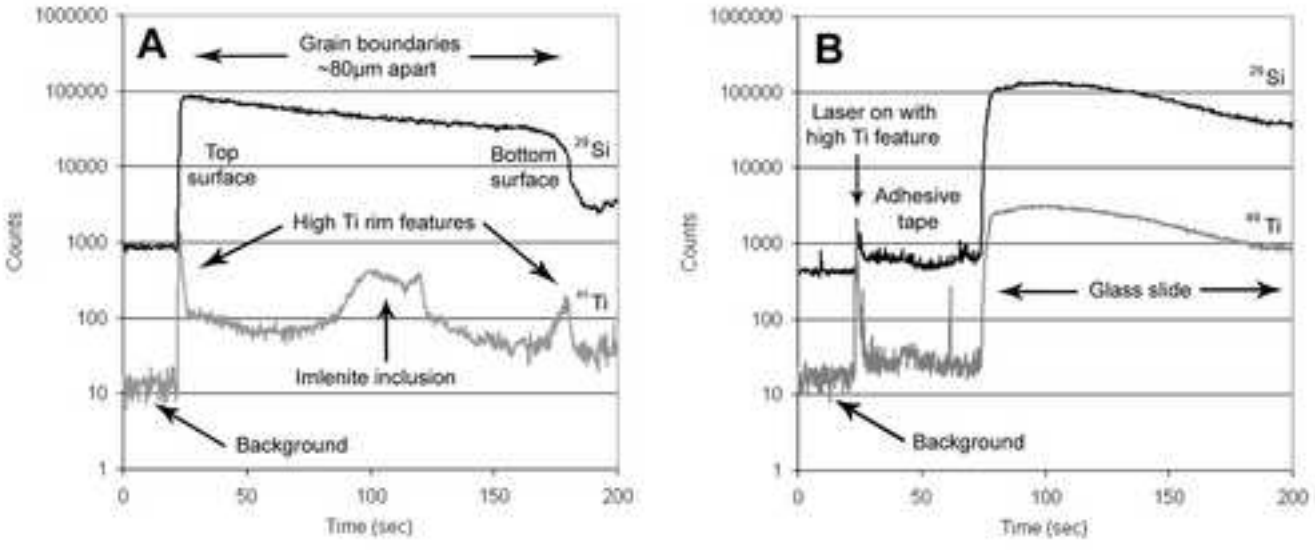

Table 1

Click here to download Table: Table_1.xls

Spot	Grain Description	Session	Order	SiO/Ti	err (%)	Ti (ppm)	err (ppm)	Temp (°C)	err (°C)	U (ppm)	Th (ppm)	Th/U	Comm 206%	204corr 238/206	err (%)	204corr 207/206	err (%)	(4) 207/206 Age (Ma)	err (1σ)	Disc (%)
G97-18R-1.1	p, m, os, mt	2	11	8873	0.6	4.8	0.3	681	12											
G97-18R-2.1	p, m, os, mt	2	12	11196	1.1	3.8	0.2	663	12											
G97-18R-3.1	p, m, os, mt	2	13	11051	0.4	3.9	0.2	664	12											
G97-18R-4.1	p, m, os, mt	2	15	9522	0.4	4.5	0.2	675	12											
G97-18R-4.2	p, c, os, mt	2	16	5638	1.2	7.6	0.4	717	14											
G97-18R-5.1	p, m, os, mt	2	17	6854	0.8	6.3	0.3	701	13											
G97-18R-5.2	p, m, os, mt	2	18	7535	0.7	5.7	0.3	694	13											
G97-18R-6.1	p, e, os, mt	2	21	10411	0.8	4.1	0.2	669	12	122	64	0.54	0.09	1.20	1.8	0.38	0.46	3820	7	-2
G97-18R-6.2	p, m, os, mt	2	22	8683	0.6	4.9	0.3	682	12											
G97-18R-7.1	p, m, os, mt	2	23	8640	0.6	5.0	0.3	683	12											
G97-18R-8.1	p, m, os, mt	2	24	6671	4.8	6.4	0.7	703	22											
G97-18R-9.1	p, m, os, mt	2	26	8680	0.7	4.9	0.3	682	12											
G97-18R-9.2	p, m, os, mt	2	27	7999	0.7	5.4	0.3	689	12											
G97-18R-10.1	p, m, os, mt	2	28	13232	0.8	3.2	0.2	651	12	172	124	0.75	0.03	1.21	1.7	0.38	0.36	3833	5	-1
G97-18R-4.3	p, m, os, mt	2	30	7316	0.9	5.9	0.3	696	13											
G97-18R-3.2	p, e, os, d	2	31	11697	0.7	3.7	0.2	660	12	148	46	0.32	0.04	1.22	1.7	0.37	0.40	3809	6	-1
G97-18R-3.3	p, m, os, mt	2	32	9390	0.5	4.6	0.2	676	12	163	58	0.37	0.05	1.22	1.7	0.37	0.50	3802	8	-1
G97-18R-3.4	p, c, rx, mt	2	33	10635	0.8	4.0	0.2	667	12											
G97-18R-2.2	p, c, os, d	2	35	2875	0.6	14.9	0.8	777	14	518	501	1.00	0.01	1.22	1.5	0.37	0.26	3811	4	-1
G97-18R-2.3	p, m, os, d	2	36	4571	1.1	9.4	0.5	735	14											
G97-18R-2.4	p, e, os, mt	2	37	17368	1.1	2.5	0.1	631	12	128	75	0.61	0.09	1.76	1.8	0.38	0.84	3825	13	32
G97-18R-7.2	p, e, os, mt	2	39	10892	0.8	3.9	0.2	665	12	167	54	0.34	0.05	1.21	1.7	0.38	0.47	3819	7	-2
G97-18R-7.3	p, c, rx, mt	2	40	8352	1.0	5.1	0.3	686	13	55	19	0.35	0.08	1.29	2.0	0.36	0.65	3741	10	1
G97-18R-6.3	p, c, os, mt	2	41	5111	0.4	8.4	0.4	726	13	179	78	0.45	0.04	1.26	1.6	0.37	0.45	3788	7	1
G97-18-11.1	p, e, os, mt	3	28	13704	1.0	3.5	0.2	656	12	204	135	0.68	0.08	1.24	1.7	0.36	2.04	3763	31	-1
G97-18-11.2	p, m, os, mt	3	29	3528	0.5	13.6	0.7	768	14											
G97-18-11.3	p, m, os, mt	3	30	12542	1.3	3.8	0.2	663	13											
G97-18-11.4	p, c, rx, l	3	31	10799	1.1	4.4	0.3	674	13	68	22	0.34	-0.09	1.28	2.0	0.36	0.61	3749	9	1
G97-18-11.5	p, m, os, mt	3	32	13291	0.7	3.6	0.2	658	12											
G97-18-11.6	p, e, os, mt	3	33	9032	1.1	5.3	0.3	688	13	136	100	0.76	0.26	1.26	1.7	0.37	0.42	3805	6	1
G97/18.12.1	p, m, os, mt	3	36	7301	0.9	6.6	0.4	705	13											
G97/18.13.1	p, c, rx, mt	3	37	19291	1.0	2.5	0.2	632	12											
G97/18.13.2	p, m, os, mt	3	38	14503	1.2	3.3	0.2	652	12											

G97/18-14.1	p, m, os, mt	3	40	10910	0.9	4.4	0.2	673	12										
G97/18-14.2	p, m, os, mt	3	41	11910	1.0	4.0	0.2	667	12										
G97/18-15.1	p, m, os, mt	3	42	9046	0.6	5.3	0.3	688	12										
G97-18R-3.5	p, m, os, mt									137	81	0.61	0.04	1.21	1.7	0.38	0.40	3832	6	-1
G97-18R-4.4	p, m, os, mt									249	166	0.69	0.04	1.19	1.6	0.38	0.45	3830	7	-2
G03-38.1	an, m, t, mt	3	6	8600	0.8	5.6	0.3	692	13	79	15	0.19	0.00	1.90	1.9	0.18	0.80	2691	13	-1
G03-38.2	ov, m, os, mt	3	7	9465	0.7	5.1	0.3	684	12	57	10	0.18	0.18	1.91	2.0	0.19	1.03	2716	17	0
G03-38.3	ov, m, h, l	3	8	10924	0.7	4.4	0.2	673	12	24	7	0.31	0.30	1.87	2.7	0.19	1.52	2736	25	-1
G03-38.4	ov, m, os, l	3	10	13006	1.0	3.7	0.2	660	12	38	9	0.23	0.12	1.74	2.0	0.19	1.68	2705	28	-8
G03-38.5	ov, m, os, mt	3	11	8456	0.5	5.7	0.3	693	12	94	26	0.29	0.15	1.84	1.7	0.19	0.53	2711	9	-3
G03-38.6	ov, e, t, mt	3	12	10459	0.7	4.6	0.2	677	12	153	49	0.33	0.09	1.93	1.7	0.19	0.59	2746	10	2
G03-38.7	ov, m, t, l	3	13	9351	0.9	5.1	0.3	685	13	47	10	0.22	0.20	1.83	1.9	0.19	0.83	2730	14	-3
G03-38.8	ov, m, t, mt	3	15	10136	0.9	4.7	0.3	679	13	71	9	0.14	0.91	1.88	1.9	0.18	2.19	2667	36	-3
G03-38.9	ov, m, t, mt	3	16	11676	0.7	4.1	0.2	668	12											
G03-38.10	eq, m, h, l	3	17	12639	0.7	3.8	0.2	662	12	36	13	0.37	0.16	1.71	2.3	0.19	0.93	2756	15	-7
G03-38.11	an, f, h, d	3	18	10653	0.7	4.5	0.2	675	12	119	16	0.14	0.02	1.85	2.3	0.19	0.57	2713	9	-3
G03-38.12	ov, m, t, mt	3	20	9415	0.7	5.1	0.3	685	12											
G03-38.14	ov, m, os, mt	3	21	10161	0.8	4.7	0.3	679	12											
G03-38.15	ov, m, t, mt	3	22	8029	0.7	6.0	0.3	697	13	72	23	0.33	0.07	1.84	2.7	0.18	2.91	2666	48	-5

Table 2

Click here to download Table: Table_2.xls

	cpx-A	gnt-A	cpx-B	gnt-B	cpx-C	gnt-C	cpx-D	gnt-D
SiO2	51.01	37.30	51.27	37.54	50.33	37.37	49.47	37.85
TiO2	0.29	0.07	0.29	0.10	0.38	0.08	0.39	0.11
Al2O3	2.30	20.69	1.97	20.74	3.06	20.84	3.46	20.44
FeO	10.72	28.95	12.60	29.93	13.27	29.28	13.41	27.94
MnO	0.16	1.01	0.24	1.34	0.26	1.03	0.25	1.04
MgO	12.26	3.80	10.47	2.91	10.23	3.72	10.50	4.00
CaO	22.30	8.38	22.96	8.45	21.78	8.49	21.10	8.79
Na2O	0.50	0.03	0.02	0.01	0.51	0.02	0.50	0.00
K2O	0.01	0.00	0.02	0.02	0.03	0.03	0.01	0.01
Cr2O3	0.03	0.06	0.07	0.08	0.04	0.02	0.07	0.00
total	99.58	100.27	99.89	101.12	99.89	100.88	99.17	100.17

Table 3

Click here to download Table: Table_3.xls

Sample	Grain Treatment	Analyses	Ti on top rim	Profiles reaching bottom rim	Ti on bottom rim	Total rims analysed	Total Ti excursions	Total Ti excursions (%)
G97-18	Untreated grain	51	45	26	21	77	66	86
G03-38	Untreated grain	5	5	5	4	10	9	90
SL13	Untreated grain	15	10	17	7	32	17	53
FC1	Untreated grain	32	25	21	11	53	36	68
Temora-2	Untreated grain	17	14	10	9	27	23	85
Temora-2	Air abraded grain	4	4	4	4	8	8	100
Temora-2	Partially HF dissolved grain	6	6	6	5	12	11	92
Temora-2	Acetone rinced grain	3	3	3	2	6	5	83
Temora-2	Ethanol rinsed grain	3	3	3	3	6	6	100
Glass		1	0					
Epoxy		2	0					
Tape		3	3					

Background Dataset 1.
Results from analysis on zircon and glass reference materials with operating conditions for each analytical session. SHRIMP SiO/Ti ratios, TiZer and LABRAT Ti concentrations used in zircon calibration.

Reference Material	Spot (SHRIMP)	Session	Order	SiO/Ti	err (%)	Ti/SiO	err (abs)	Ti (ppm) (TiZer)	err (ppm)	Spot (LA-ICPMS)	Ti (ppm) (LABRAT)	err (ppm)
SL13	SL13-1.1	1	47	7391	0.3	0.0001353	0.0000004	6.1	0.4			
SL13	SL13-1.2	1	48	7334	0.6	0.0001364	0.0000008	6.2	0.4			
SL13	SL13-2.1	1	49	7892	0.5	0.0001267	0.0000006	5.7	0.3			
SL13	SL13-2.2	1	50	7523	0.5	0.0001329	0.0000007	6.0	0.4			
SL13	SL13-3.1	1	51	7186	0.4	0.0001392	0.0000006	6.3	0.4			
SL13	SL13-3.2	1	52	7053	0.4	0.0001418	0.0000006	6.4	0.4			
SL13	SL13-4.1	1	53	7592	0.4	0.0001317	0.0000005	6.0	0.3			
SL13	SL13-4.2	1	54	7391	0.3	0.0001353	0.0000004	6.1	0.4			
SL13	SL13-5.1	1	55	6654	0.5	0.0001503	0.0000008	6.8	0.4			
SL13	SL13-5.2	1	56	6892	0.3	0.0001451	0.0000004	6.6	0.4			
SL13	SL13-6.1	1	57	7653	0.5	0.0001307	0.0000007	5.9	0.3			
SL13	SL13-6.2	1	58	7466	0.5	0.0001339	0.0000007	6.1	0.4			
SL13	SL13-1.1	2	1	6919	0.6	0.0001445	0.0000009	6.2	0.3	J07-SL13-1.0	6.3	0.5
SL13	SL13-1.2	2	2	7071	0.7	0.0001414	0.0000010	6.1	0.3			
SL13	SL13-1.3	2	7	7013	0.4	0.0001426	0.0000006	6.1	0.3			
SL13	SL13-2.1	2	14	7043	0.6	0.0001420	0.0000009	6.1	0.3	J10-SL13-2.6	6.4	0.5
SL13	SL13-2.2	2	19	7080	0.7	0.0001412	0.0000010	6.1	0.3			
SL13	SL13-2.2	2	20	7021	0.4	0.0001424	0.0000006	6.1	0.3			
SL13	SL13-1.4	2	25	6999	0.6	0.0001429	0.0000009	6.1	0.3	J05-SL13-1.4	6.5	0.6
SL13	SL13-1.5	2	29	7079	0.6	0.0001413	0.0000008	6.1	0.3			
SL13	SL13-1.6	2	34	6996	0.6	0.0001429	0.0000009	6.1	0.3			
SL13	SL13-1.7	2	38	7032	0.5	0.0001422	0.0000007	6.1	0.3	J06-SL13-1.7	6.3	0.5
SL13	SL13-1.8	2	42	7067	0.6	0.0001415	0.0000008	6.1	0.3			

SL13	SL13-1.9	2	46	6966	0.4	0.0001436	0.0000006	6.2	0.3			
SL13	SL13-2.3	2	51	6944	0.5	0.0001440	0.0000007	6.2	0.3			
SL13	SL13-2.4	2	56	6934	0.4	0.0001442	0.0000006	6.2	0.3	J14-SL13-2.4	6.4	0.5
SL13	SL13-2.5	2	61	6858	0.7	0.0001458	0.0000010	6.3	0.3	J13-SL13-2.5	6.5	0.5
SL13	SL13-1.9	2	66	6812	0.8	0.0001468	0.0000012	6.3	0.3	J04-SL13-1.9	6.4	0.6
SL13	SL13-1.9	2	67	6810	0.4	0.0001468	0.0000006	6.3	0.3			
SL13	SL13-2.6	2	72	6823	0.5	0.0001466	0.0000007	6.3	0.3			
SL13	SL13-3.1	2	80	7096	0.7	0.0001409	0.0000010	6.0	0.3			
SL13	SL13-3.2	2	81	7119	0.7	0.0001405	0.0000010	6.0	0.3			
SL13	SL13-3.3	2	86	7177	0.5	0.0001393	0.0000007	6.0	0.3			
SL13	SL13-2.7	2	90	7058	0.5	0.0001417	0.0000007	6.1	0.3			
SL13	SL13-2.8	2	95	7013	0.7	0.0001426	0.0000010	6.1	0.3	J11-SL13-2.8	6.4	0.5
SL13	SL13-3.4	2	99	7152	0.3	0.0001398	0.0000004	6.0	0.3			
SL13	SL13-2.9	2	100	6889	0.6	0.0001452	0.0000009	6.2	0.3			
SL13	SL13-2.10	2	105	6794	0.5	0.0001472	0.0000007	6.3	0.3			
SL13	SL13-1.10	3	1	7033	0.6	0.0001422	0.0000009	6.1	0.3	J03-SL13-1.1	6.4	0.6
SL13	SL13-1.11	3	2	6964	0.4	0.0001436	0.0000006	6.2	0.3			
SL13	SL13-2.10	3	6	7033	0.8	0.0001422	0.0000011	6.1	0.3	J12-SL13-2.0	6.4	0.5
SL13	SL13.1	4	5	7824	0.6	0.0001278	0.0000008	6.1	0.3			
SL13	SL13.2	4	9	7709	0.6	0.0001297	0.0000008	6.2	0.3			
SL13	SL13.3	4	14	7721	0.6	0.0001295	0.0000008	6.2	0.3			
SL13	SL13.4	4	19	7637	0.9	0.0001309	0.0000012	6.3	0.3			
SL13	SL13.5	4	23	8040	0.7	0.0001244	0.0000009	6.0	0.3			
SL13	SL13.7	4	24	7830	1.0	0.0001277	0.0000013	6.1	0.3			
SL13	SL13.9	4	25	7835	0.8	0.0001276	0.0000010	6.1	0.3			
SL13	SL13.9B	4	26	8048	0.6	0.0001243	0.0000007	5.9	0.3			
SL13	SL13.9C	4	27	7747	0.9	0.0001291	0.0000012	6.2	0.3			
SL13	SL13.10	4	35	7940	0.8	0.0001259	0.0000010	6.0	0.3			
SL13	SL13.11	4	39	7825	0.5	0.0001278	0.0000006	6.1	0.3			
SL13	SL13.12	4	43	7636	0.6	0.0001310	0.0000008	6.3	0.3			

SL13	SL13-3.1	5	275	6873	1.6	0.0001455	0.0000023	6.0	0.4			
SL13	SL13-3.2	5	276	6795	1.2	0.0001472	0.0000018	6.1	0.4			
SL13	SL13-3.3	5	277	7011	1.0	0.0001426	0.0000014	5.9	0.4			
SL13	SL13-3.4	5	437	6702	1.6	0.0001492	0.0000024	6.2	0.4			
SL13	SL13-3.5	5	469	6453	2.3	0.0001550	0.0000036	6.4	0.5			
SL13	SL13-3.6	5	1073	7200	1.2	0.0001389	0.0000017	5.8	0.4			
SL13	SL13-3.7	5	1074	6796	1.3	0.0001471	0.0000019	6.1	0.4			
SL13	SL13-3.8	5	1075	6470	1.3	0.0001546	0.0000020	6.4	0.4			
SL13	SL13-3.9	5	1076	7098	0.8	0.0001409	0.0000011	5.9	0.4			
SL13	SL13-3.10	5	1077	6890	0.4	0.0001451	0.0000006	6.0	0.4			
SL13	SL13-2.1	5	1515	6005	2.1	0.0001665	0.0000035	6.9	0.5			
Temora-2	TEM-1.1	1	31	6797	0.4	0.0001471	0.0000006	6.6	0.4			
Temora-2	TEM-1.2	1	32	6550	0.5	0.0001527	0.0000008	6.9	0.4			
Temora-2	TEM-1.3	1	33	6453	0.5	0.0001550	0.0000008	7.0	0.4			
Temora-2	TEM-2.1	1	34	6221	0.3	0.0001607	0.0000005	7.3	0.4			
Temora-2	TEM-2.2	1	35	6592	0.4	0.0001517	0.0000006	6.9	0.4			
Temora-2	TEM-2.3	1	36	6589	0.4	0.0001518	0.0000006	6.9	0.4			
Temora-2	TEM-2.4	1	37	5803	0.4	0.0001723	0.0000007	7.8	0.4			
Temora-2	TEM-3.1	1	39	5029	0.4	0.0001988	0.0000008	9.0	0.5			
Temora-2	TEM-3.2	1	40	3906	0.8	0.0002560	0.0000020	11.6	0.7			
Temora-2	TEM-4.1	1	41	4763	0.2	0.0002100	0.0000004	9.5	0.5			
Temora-2	TEM-2.1	2	4	4923	0.7	0.0002031	0.0000014	8.7	0.5	J17-TEM-2.1	8.9	0.7
Temora-2	TEM-1.2	2	5	4552	0.3	0.0002197	0.0000007	9.4	0.5	J18-TEM-1.2	9.3	0.8
Temora-2	TEM-3.1	2	6	5478	0.3	0.0001825	0.0000005	7.8	0.4	J21-TEM-3.2	8.4	0.7
Temora-2	TEM-4.1	2	77	4610	0.6	0.0002169	0.0000013	9.3	0.5	J22-TEM-4.1	9.2	0.8
Temora-2	TEM-5.1	2	78	4438	0.5	0.0002253	0.0000011	9.7	0.5	J23-TEM-5.1	10.2	0.9
Temora-2	TEM-6.1	2	79	5414	0.3	0.0001847	0.0000006	7.9	0.4	J24-TEM-6.1	8.2	0.7
FC1	FC1-1.1	1	22	3524	0.2	0.0002838	0.0000006	12.8	0.7			

FC1	FC1-2.1	1	24	3841	0.3	0.0002603	0.0000008	11.8	0.7			
FC1	FC1-2.2	1	25	3828	0.2	0.0002612	0.0000005	11.8	0.7			
FC1	FC1-2.3	1	26	4124	0.5	0.0002425	0.0000012	11.0	0.6			
FC1	FC1-3.1	1	28	4021	0.3	0.0002487	0.0000007	11.2	0.6			
FC1	FC1-3.2	1	29	3608	0.3	0.0002772	0.0000008	12.5	0.7			
FC1	FC1-1.1	2	8	1942	0.4	0.0005149	0.0000021	22.1	1.1	J28-FC1-1.1	24.0	1.9
FC1	FC1-1.2	2	9	2044	0.3	0.0004892	0.0000015	21.0	1.1	J27-FC1-1.2	22.3	1.9
FC1	FC1-2.1	2	10	1763	0.4	0.0005672	0.0000023	24.3	1.2	J30-FC1-2.1	25.3	2.0
FC1	FC1-3.1	2	73	1823	0.4	0.0005485	0.0000022	23.5	1.2	J29-FC1-3.1	21.4	1.8
FC1	FC1-4.1	2	74	2266	0.2	0.0004413	0.0000009	18.9	1.0	J31-FC1-4.1	18.5	1.5
FC1	FC1-5.1	2	75	1822	0.3	0.0005488	0.0000016	23.5	1.2	J32-FC1-5.1	20.4	1.7
FC1	FC1-6.1	2	76	2156	0.3	0.0004638	0.0000014	19.9	1.0	J33-FC1-6.1	22.0	1.8
NIST 610	NIST 610-1.1	1	13	2663	0.0	0.0003755	0.0000000					
NIST 610	NIST 610-2.1	1	14	2601	0.1	0.0003845	0.0000004					
NIST 610	NIST 610-2.2	1	15	2535	0.1	0.0003945	0.0000004					
NIST 610	NIST 610-3.1	1	16	2471	0.1	0.0004047	0.0000004					
NIST 610	NIST 610-3.2	1	17	2408	0.1	0.0004153	0.0000004					
NIST 610	NIST 610-3.3	1	18	2344	0.1	0.0004266	0.0000004					
NIST 610	NIST 610-3.3	1	19	2275	0.1	0.0004396	0.0000004					
NIST 610	NIST 610-3.3	1	20	2206	0.1	0.0004533	0.0000005					
NIST 610	NIST 610-3.3	1	21	2138	0.2	0.0004677	0.0000009					
NIST 610	NIST 610-3.4	1	23	2025	0.1	0.0004938	0.0000005					
NIST 612	NIST 612-1.1	1	7	5313	0.2	0.0001882	0.0000004					
NIST 612	NIST 612-1.2	1	8	5251	0.2	0.0001904	0.0000004					
NIST 612	NIST 612-1.3	1	9	5216	0.3	0.0001917	0.0000006					
NIST 612	NIST 612-2.1	1	10	5122	0.2	0.0001952	0.0000004					
NIST 612	NIST 612-2.2	1	11	5053	0.2	0.0001979	0.0000004					
NIST 612	NIST 612-2.3	1	12	5010	0.3	0.0001996	0.0000006					

NIST 615	NIST 615-1.1	1	1	39611	1.0	0.0000252	0.0000003
NIST 615	NIST 615-1.2	1	2	39192	0.7	0.0000255	0.0000002
NIST 615	NIST 615-2.1	1	3	39198	0.7	0.0000255	0.0000002
NIST 615	NIST 615-2.2	1	4	40161	1.3	0.0000249	0.0000003
NIST 615	NIST 615-2.3	1	5	39294	0.6	0.0000254	0.0000002
NIST 615	NIST 615-2.4	1	6	39207	0.8	0.0000255	0.0000002
NIST 615	NIST 615-1.3	1	44	36317	0.8	0.0000275	0.0000002
NIST 615	NIST 615-1.3	1	45	36255	0.9	0.0000276	0.0000002
NIST 615	NIST 615-1.4	1	46	36898	0.7	0.0000271	0.0000002
NIST 615	NIST 615-1.5	1	59	35523	1.0	0.0000282	0.0000003

Background Dataset 2.
SHRIMP SiO/Ti ratios, TiZer Ti concentrations and temperatures from matrix mapping of grains G97/18-2, G97/18-11 and FC1-7 during session 5.

Grain	Block	Spot	Order	SiO/Ti	err (%)	Ti (ppm)	err (ppm)	Temp (°C)	err (°C)
G97-18-2	A	1_8	1078	6071	2.5	6.8	0.5	709	17
G97-18-2	A	1_9	1079	133	4.6	311.3	70.6	1171	94
G97-18-2	A	1_10	1080	961	11.8	43.2	12.5	888	77
G97-18-2	A	2_5	1081	4639	13.7	9.0	2.6	731	58
G97-18-2	A	2_6	1082	9691	4.1	4.3	0.5	672	20
G97-18-2	A	2_7	1083	11023	2.4	3.8	0.3	662	16
G97-18-2	A	2_8	1084	9627	1.7	4.3	0.3	672	15
G97-18-2	A	2_9	1085	7012	1.7	5.9	0.4	697	15
G97-18-2	A	2_10	1086	3218	2.3	12.9	1.0	764	19
G97-18-2	A	2_11	1087	677	5.5	61.3	9.4	930	45
G97-18-2	A	2_12	1088	357	1.0	116.4	7.6	1015	25
G97-18-2	A	3_4	1089	10376	6.0	4.0	0.6	666	26
G97-18-2	A	3_5	1090	12721	1.4	3.3	0.3	651	15
G97-18-2	A	3_6	1091	11301	2.2	3.7	0.3	660	16
G97-18-2	A	3_7	1092	12048	1.5	3.5	0.3	655	15
G97-18-2	A	3_8	1093	12877	0.6	3.2	0.3	650	15
G97-18-2	A	3_9	1094	11655	1.1	3.6	0.3	658	15
G97-18-2	A	3_10	1095	8267	0.4	5.0	0.3	684	14
G97-18-2	A	3_11	1096	2953	1.9	14.1	1.0	772	18
G97-18-2	A	3_12	1097	872	6.8	47.6	8.4	900	49
G97-18-2	A	3_13	1098	468	6.1	88.7	16.1	978	57
G97-18-2	A	4_3	1100	651	9.1	63.8	15.6	935	71
G97-18-2	A	4_4	1101	2122	2.2	19.6	1.5	804	20
G97-18-2	A	4_5	1102	10177	0.9	4.1	0.3	668	14
G97-18-2	A	4_6	1103	12674	1.4	3.3	0.3	652	15
G97-18-2	A	4_7	1104	14848	2.5	2.8	0.3	640	18
G97-18-2	A	4_8	1105	16061	1.7	2.6	0.2	635	17
G97-18-2	A	4_9	1106	15875	1.7	2.6	0.2	635	17
G97-18-2	A	4_10	1107	14920	1.4	2.8	0.2	640	16
G97-18-2	A	4_11	1108	10794	1.6	3.9	0.3	663	15
G97-18-2	A	4_12	1109	4320	4.5	9.6	1.1	737	24
G97-18-2	A	4_13	1110	709	9.3	58.5	14.3	924	70
G97-18-2	A	4_15	1112	73	15.9	571.5	681.9	1289	573
G97-18-2	A	5_3	1113	10215	7.4	4.1	0.7	668	30
G97-18-2	A	5_4	1114	13939	1.2	3.0	0.3	645	16
G97-18-2	A	5_5	1115	14499	2.6	2.9	0.3	642	18
G97-18-2	A	5_6	1116	17806	1.3	2.3	0.2	627	17
G97-18-2	A	5_7	1117	20508	2.0	2.0	0.2	618	19
G97-18-2	A	5_8	1118	19085	2.3	2.2	0.2	623	19
G97-18-2	A	5_9	1119	17103	2.4	2.4	0.3	630	18

G97-18-2	A	5_10	1120	14826	1.8	2.8	0.3	640	17
G97-18-2	A	5_11	1121	13033	1.2	3.2	0.3	650	15
G97-18-2	A	5_12	1122	12063	1.5	3.4	0.3	655	15
G97-18-2	A	5_13	1123	4583	4.1	9.1	0.9	732	22
G97-18-2	A	5_14	1124	717	15.3	58.0	23.0	923	112
G97-18-2	A	5_15	1125	1131	1.2	36.7	2.4	870	20
G97-18-2	A	6_2	1126	9193	2.9	4.5	0.4	676	17
G97-18-2	A	6_3	1127	13255	3.2	3.1	0.3	648	19
G97-18-2	A	6_4	1128	13742	2.5	3.0	0.3	646	17
G97-18-2	A	6_5	1129	17610	0.4	2.4	0.2	628	17
G97-18-2	A	6_6	1130	20500	2.2	2.0	0.2	618	19
G97-18-2	A	6_7	1131	19362	1.6	2.1	0.2	622	18
G97-18-2	A	6_8	1132	15806	1.1	2.6	0.2	636	16
G97-18-2	A	6_9	1133	13377	1.8	3.1	0.3	648	16
G97-18-2	A	6_10	1134	12672	0.6	3.3	0.3	652	15
G97-18-2	A	6_11	1135	11315	1.1	3.7	0.3	660	15
G97-18-2	A	6_12	1136	11973	0.4	3.5	0.3	656	15
G97-18-2	A	6_13	1137	13805	0.9	3.0	0.2	645	15
G97-18-2	A	6_14	1138	9856	2.1	4.2	0.3	670	16
G97-18-2	A	6_15	1139	4275	1.1	9.7	0.6	738	15
G97-18-2	A	7_2	1140	5674	7.9	7.3	1.3	714	35
G97-18-2	A	7_3	1141	10085	0.5	4.1	0.3	669	14
G97-18-2	A	7_4	1142	13544	1.5	3.1	0.3	647	16
G97-18-2	A	7_5	1143	17706	1.4	2.4	0.2	628	17
G97-18-2	A	7_6	1144	19983	2.1	2.1	0.2	619	19
G97-18-2	A	7_7	1145	18543	2.2	2.2	0.2	625	18
G97-18-2	A	7_8	1146	18691	0.8	2.2	0.2	624	17
G97-18-2	A	7_9	1147	13744	2.0	3.0	0.3	646	16
G97-18-2	A	7_10	1148	12536	0.8	3.3	0.3	652	15
G97-18-2	A	7_11	1149	13094	1.7	3.2	0.3	649	16
G97-18-2	A	7_12	1150	12059	1.9	3.4	0.3	655	16
G97-18-2	A	7_13	1151	13119	0.4	3.2	0.2	649	15
G97-18-2	A	7_14	1152	13442	1.9	3.1	0.3	647	16
G97-18-2	A	7_15	1153	9841	1.1	4.2	0.3	670	15
G97-18-2	A	8_2	1154	7298	2.0	5.7	0.4	694	16
G97-18-2	A	8_3	1155	9325	1.9	4.5	0.3	675	16
G97-18-2	A	8_4	1156	13287	1.8	3.1	0.3	648	16
G97-18-2	A	8_5	1157	18190	2.1	2.3	0.2	626	18
G97-18-2	A	8_6	1158	17757	1.5	2.3	0.2	628	17
G97-18-2	A	8_7	1159	17219	2.5	2.4	0.3	630	18
G97-18-2	A	8_8	1160	18738	2.3	2.2	0.2	624	18
G97-18-2	A	8_9	1161	12943	0.9	3.2	0.3	650	15
G97-18-2	A	8_10	1162	13304	0.9	3.1	0.3	648	15
G97-18-2	A	8_11	1163	13095	1.5	3.2	0.3	649	16
G97-18-2	A	8_12	1164	11162	1.3	3.7	0.3	661	15
G97-18-2	A	8_13	1165	11523	2.2	3.6	0.3	659	16

G97-18-2	A	8_14	1166	11383	1.4	3.7	0.3	659	15
G97-18-2	A	8_15	1167	10267	1.9	4.0	0.3	667	16
G97-18-2	A	9_2	1168	8635	3.8	4.8	0.5	680	20
G97-18-2	A	9_3	1169	10660	1.0	3.9	0.3	664	15
G97-18-2	A	9_4	1170	13867	1.5	3.0	0.3	645	16
G97-18-2	A	9_5	1171	18074	3.6	2.3	0.3	626	20
G97-18-2	A	9_6	1172	19067	1.2	2.2	0.2	623	18
G97-18-2	A	9_7	1173	18185	2.5	2.3	0.3	626	19
G97-18-2	A	9_8	1174	16341	1.5	2.5	0.2	633	17
G97-18-2	A	9_9	1175	11613	1.1	3.6	0.3	658	15
G97-18-2	A	9_10	1176	12073	1.2	3.4	0.3	655	15
G97-18-2	A	9_11	1177	10290	2.1	4.0	0.3	667	16
G97-18-2	A	9_12	1178	8491	1.5	4.9	0.3	682	15
G97-18-2	A	9_13	1179	8373	1.0	5.0	0.3	683	14
G97-18-2	A	9_14	1180	9056	0.7	4.6	0.3	677	14
G97-18-2	A	9_15	1181	9449	1.4	4.4	0.3	674	15
G97-18-2	A	10_2	1182	9428	5.2	4.4	0.6	674	23
G97-18-2	A	10_3	1183	10613	2.8	3.9	0.4	665	17
G97-18-2	A	10_4	1184	12308	2.2	3.4	0.3	654	16
G97-18-2	A	10_5	1185	15606	1.8	2.7	0.3	637	17
G97-18-2	A	10_6	1186	16625	1.3	2.5	0.2	632	17
G97-18-2	A	10_7	1187	17879	0.5	2.3	0.2	627	17
G97-18-2	A	10_8	1188	14603	1.8	2.8	0.3	641	17
G97-18-2	A	10_9	1189	10685	0.8	3.9	0.3	664	14
G97-18-2	A	10_10	1190	9772	2.2	4.3	0.3	671	16
G97-18-2	A	10_11	1191	5664	1.6	7.3	0.5	714	15
G97-18-2	A	10_12	1192	6405	2.2	6.5	0.5	704	16
G97-18-2	A	10_13	1193	6230	0.4	6.7	0.4	707	14
G97-18-2	A	10_14	1194	5687	0.8	7.3	0.4	714	14
G97-18-2	A	10_15	1195	6248	0.8	6.7	0.4	706	14
G97-18-2	A	11_2	1196	2549	5.2	16.3	2.1	786	30
G97-18-2	A	11_3	1197	5930	1.7	7.0	0.5	711	15
G97-18-2	A	11_4	1198	10039	1.0	4.1	0.3	669	14
G97-18-2	A	11_5	1199	13724	1.4	3.0	0.3	646	16
G97-18-2	A	11_6	1200	14607	0.5	2.8	0.2	641	15
G97-18-2	A	11_7	1201	16706	2.0	2.5	0.2	632	17
G97-18-2	A	11_8	1202	14640	2.7	2.8	0.3	641	18
G97-18-2	A	11_9	1203	10299	1.1	4.0	0.3	667	15
G97-18-2	A	11_10	1204	5173	4.6	8.0	0.9	722	24
G97-18-2	A	11_11	1205	6247	2.1	6.7	0.5	706	16
G97-18-2	A	11_12	1206	6490	1.2	6.4	0.4	703	14
G97-18-2	A	11_13	1207	4277	1.1	9.7	0.6	738	15
G97-18-2	A	11_14	1208	3313	0.3	12.5	0.7	761	15
G97-18-2	A	11_15	1209	4349	0.7	9.6	0.6	737	15
G97-18-2	A	12_3	1210	5200	1.1	8.0	0.5	722	15
G97-18-2	A	12_4	1211	9468	1.0	4.4	0.3	673	14

G97-18-2	A	12_5	1212	11148	1.7	3.7	0.3	661	15
G97-18-2	A	12_6	1213	12806	1.5	3.2	0.3	651	16
G97-18-2	A	12_7	1214	13120	1.4	3.2	0.3	649	16
G97-18-2	A	12_8	1215	11356	1.1	3.7	0.3	660	15
G97-18-2	A	12_9	1216	9966	0.4	4.2	0.3	669	14
G97-18-2	A	12_10	1217	8957	1.0	4.6	0.3	678	14
G97-18-2	A	12_11	1218	7680	0.9	5.4	0.3	690	14
G97-18-2	A	12_12	1219	5741	1.9	7.2	0.5	713	16
G97-18-2	A	12_13	1220	3094	0.7	13.4	0.8	768	16
G97-18-2	A	12_14	1221	2795	3.1	14.9	1.3	777	21
G97-18-2	A	12_15	1222	3227	1.6	12.9	0.9	764	17
G97-18-2	A	13_3	1223	3987	2.4	10.4	0.8	745	18
G97-18-2	A	13_4	1224	6356	1.7	6.5	0.5	705	15
G97-18-2	A	13_5	1225	9552	0.6	4.4	0.3	673	14
G97-18-2	A	13_6	1226	12941	1.1	3.2	0.3	650	15
G97-18-2	A	13_7	1227	13773	1.8	3.0	0.3	646	16
G97-18-2	A	13_8	1228	11127	1.2	3.7	0.3	661	15
G97-18-2	A	13_9	1229	9767	1.7	4.3	0.3	671	15
G97-18-2	A	13_10	1230	9347	0.5	4.4	0.3	674	14
G97-18-2	A	13_11	1231	8865	0.9	4.7	0.3	678	14
G97-18-2	A	13_12	1232	7743	0.7	5.4	0.3	689	14
G97-18-2	A	13_13	1233	3631	0.5	11.4	0.7	753	15
G97-18-2	A	13_14	1234	3164	0.8	13.1	0.8	765	16
G97-18-2	A	13_15	1235	2919	0.6	14.2	0.9	773	16
G97-18-2	A	14_4	1236	2646	8.3	15.7	3.0	782	43
G97-18-2	A	14_5	1237	7438	1.0	5.6	0.4	692	14
G97-18-2	A	14_6	1238	9918	1.4	4.2	0.3	670	15
G97-18-2	A	14_7	1239	13240	1.5	3.1	0.3	648	16
G97-18-2	A	14_8	1240	13383	2.1	3.1	0.3	648	17
G97-18-2	A	14_9	1241	12266	1.6	3.4	0.3	654	16
G97-18-2	A	14_10	1242	12563	1.0	3.3	0.3	652	15
G97-18-2	A	14_11	1243	12091	1.4	3.4	0.3	655	15
G97-18-2	A	14_12	1244	10448	2.0	4.0	0.3	666	16
G97-18-2	A	14_13	1245	6692	1.5	6.2	0.4	701	15
G97-18-2	A	14_14	1246	4456	0.2	9.3	0.6	735	14
G97-18-2	A	14_15	1247	4139	0.4	10.0	0.6	741	15
G97-18-2	A	15_5	1248	3246	1.0	12.8	0.8	763	16
G97-18-2	A	15_6	1249	5506	1.5	7.5	0.5	717	15
G97-18-2	A	15_7	1250	8027	2.3	5.2	0.4	686	16
G97-18-2	A	15_8	1251	11088	1.7	3.7	0.3	661	15
G97-18-2	A	15_9	1252	14093	0.9	3.0	0.2	644	16
G97-18-2	A	15_10	1253	15145	0.4	2.7	0.2	639	16
G97-18-2	A	15_11	1254	14124	0.7	2.9	0.2	644	15
G97-18-2	A	15_12	1255	12307	1.2	3.4	0.3	654	15
G97-18-2	A	15_13	1256	10317	1.1	4.0	0.3	667	15
G97-18-2	A	15_14	1257	8191	0.9	5.1	0.3	685	14

G97-18-2	A	15_15	1258	6025	0.6	6.9	0.4	709	14
G97-18-2	A	16_7	1259	3819	3.3	10.9	1.0	748	21
G97-18-2	A	16_8	1260	6100	2.0	6.8	0.5	708	16
G97-18-2	A	16_9	1261	5676	3.5	7.3	0.7	714	20
G97-18-2	A	16_10	1262	8196	2.7	5.1	0.4	685	17
G97-18-2	A	16_11	1263	13233	0.6	3.1	0.3	648	15
G97-18-2	A	16_12	1264	11991	2.3	3.5	0.3	656	17
G97-18-2	A	16_13	1265	11749	0.8	3.5	0.3	657	15
G97-18-2	A	16_14	1266	11246	1.0	3.7	0.3	660	15
G97-18-2	A	16_15	1267	9249	0.7	4.5	0.3	675	14
G97-18-2	A	17_8	1268	986	4.3	42.1	5.3	885	35
G97-18-2	A	17_9	1269	3568	3.0	11.6	1.0	754	20
G97-18-2	A	17_10	1270	6481	2.8	6.4	0.5	703	18
G97-18-2	A	17_11	1271	8722	1.4	4.8	0.3	680	15
G97-18-2	A	17_12	1272	11913	0.6	3.5	0.3	656	15
G97-18-2	A	17_13	1273	14350	1.2	2.9	0.2	643	16
G97-18-2	A	17_14	1274	13110	0.8	3.2	0.3	649	15
G97-18-2	A	17_15	1275	11617	0.6	3.6	0.3	658	15
G97-18-2	A	18_10	1276	2439	3.0	17.0	1.5	790	22
G97-18-2	A	18_11	1277	5350	0.9	7.8	0.5	719	15
G97-18-2	A	18_12	1278	8589	0.7	4.8	0.3	681	14
G97-18-2	A	18_13	1279	9755	2.2	4.3	0.3	671	16
G97-18-2	A	18_14	1280	13655	1.3	3.0	0.3	646	16
G97-18-2	A	18_15	1281	13236	1.1	3.1	0.3	648	15
G97-18-2	A	19_12	1282	4352	0.6	9.5	0.6	737	15
G97-18-2	A	19_13	1283	7176	2.0	5.8	0.4	695	16
G97-18-2	A	19_14	1284	10178	1.1	4.1	0.3	668	15
G97-18-2	A	19_15	1285	12059	1.5	3.4	0.3	655	15
G97-18-2	A	20_13	1286	3050	5.2	13.6	1.7	769	29
G97-18-2	A	20_14	1287	7514	1.3	5.5	0.4	691	14
G97-18-2	A	20_15	1288	10698	1.3	3.9	0.3	664	15
G97-18-2	B	1_1	1289	1505	3.8	27.6	3.0	839	28
G97-18-2	B	1_2	1290	628	2.2	66.1	5.7	940	27
G97-18-2	B	1_3	1291	385	4.3	107.8	17.4	1004	53
G97-18-2	B	2_1	1292	4079	0.6	10.2	0.6	743	15
G97-18-2	B	2_2	1293	2393	0.2	17.4	1.0	792	16
G97-18-2	B	2_3	1294	1180	3.2	35.2	3.5	865	27
G97-18-2	B	2_4	1295	208	3.0	200.1	31.3	1097	59
G97-18-2	B	3_1	1296	8625	1.4	4.8	0.3	681	15
G97-18-2	B	3_2	1297	6041	1.8	6.9	0.5	709	16
G97-18-2	B	3_3	1298	2772	2.2	15.0	1.1	778	19
G97-18-2	B	3_4	1299	1030	8.6	40.3	9.2	880	61
G97-18-2	B	3_5	1300	862	1.8	48.2	3.7	901	23
G97-18-2	B	3_6	1301	672	5.1	61.8	9.7	931	46
G97-18-2	B	4_1	1302	8752	1.4	4.7	0.3	679	15
G97-18-2	B	4_2	1303	10189	1.7	4.1	0.3	668	15

G97-18-2	B	4_3	1304	7529	1.5	5.5	0.4	691	15
G97-18-2	B	4_4	1305	3451	1.0	12.0	0.8	757	16
G97-18-2	B	4_5	1306	2204	0.7	18.8	1.1	800	17
G97-18-2	B	4_6	1307	1250	1.4	33.2	2.3	859	20
G97-18-2	B	4_7	1308	312	13.6	133.2	70.6	1034	179
G97-18-2	B	5_1	1309	8209	1.3	5.1	0.3	684	15
G97-18-2	B	5_2	1310	9496	1.8	4.4	0.3	673	15
G97-18-2	B	5_3	1311	10409	1.7	4.0	0.3	666	15
G97-18-2	B	5_4	1312	10458	1.7	4.0	0.3	666	15
G97-18-2	B	5_5	1313	5388	0.9	7.7	0.5	719	15
G97-18-2	B	5_6	1314	2126	2.0	19.5	1.4	803	19
G97-18-2	B	5_7	1315	203	4.2	204.1	44.1	1100	81
G97-18-2	B	5_9	1317	144	2.7	288.4	51.0	1158	73
G97-18-2	B	6_1	1318	5168	1.1	8.0	0.5	722	15
G97-18-2	B	6_2	1319	6848	0.7	6.1	0.4	699	14
G97-18-2	B	6_3	1320	9432	0.6	4.4	0.3	674	14
G97-18-2	B	6_4	1321	10395	1.3	4.0	0.3	666	15
G97-18-2	B	6_5	1322	11718	1.4	3.5	0.3	657	15
G97-18-2	B	6_6	1323	9929	1.7	4.2	0.3	670	15
G97-18-2	B	6_7	1324	2966	0.9	14.0	0.9	771	16
G97-18-2	B	6_8	1325	2206	1.5	18.8	1.3	800	18
G97-18-2	B	6_9	1326	460	0.7	90.3	5.6	980	23
G97-18-2	B	6_10	1327	300	14.5	138.2	80.9	1040	199
G97-18-2	B	7_1	1328	2810	0.7	14.8	0.9	776	16
G97-18-2	B	7_2	1329	3840	0.3	10.8	0.6	748	15
G97-18-2	B	7_3	1330	6573	1.6	6.3	0.4	702	15
G97-18-2	B	7_4	1331	9344	1.7	4.4	0.3	674	15
G97-18-2	B	7_5	1332	11504	1.7	3.6	0.3	659	16
G97-18-2	B	7_6	1333	13759	0.8	3.0	0.2	646	15
G97-18-2	B	7_7	1334	16529	2.0	2.5	0.3	633	17
G97-18-2	B	7_8	1335	9630	1.9	4.3	0.3	672	15
G97-18-2	B	7_9	1336	4221	1.3	9.8	0.6	740	16
G97-18-2	B	7_10	1337	2412	0.5	17.2	1.0	791	16
G97-18-2	B	7_11	1338	1244	2.6	33.4	2.9	859	24
G97-18-2	B	7_12	1339	707	5.4	58.7	9.7	925	48
G97-18-2	B	8_1	1340	2233	1.0	18.6	1.2	799	17
G97-18-2	B	8_2	1341	2982	0.6	13.9	0.8	771	16
G97-18-2	B	8_3	1342	5734	0.9	7.2	0.4	713	14
G97-18-2	B	8_4	1343	8568	0.6	4.9	0.3	681	14
G97-18-2	B	8_5	1344	10755	1.0	3.9	0.3	664	15
G97-18-2	B	8_6	1345	13215	1.2	3.1	0.3	648	15
G97-18-2	B	8_7	1346	16001	2.0	2.6	0.3	635	17
G97-18-2	B	8_8	1347	18038	1.4	2.3	0.2	626	17
G97-18-2	B	8_9	1348	13253	2.4	3.1	0.3	648	17
G97-18-2	B	8_10	1349	6302	1.2	6.6	0.4	706	14
G97-18-2	B	8_11	1350	3233	1.7	12.8	0.9	763	17

G97-18-2	B	8_12	1351	431	34.0	96.3	113.5	989	369
G97-18-2	B	9_1	1353	3321	1.4	12.5	0.8	761	16
G97-18-2	B	9_2	1354	4398	0.4	9.4	0.6	736	15
G97-18-2	B	9_3	1355	6463	0.6	6.4	0.4	704	14
G97-18-2	B	9_4	1356	7327	1.2	5.7	0.4	693	14
G97-18-2	B	9_5	1357	8816	0.9	4.7	0.3	679	14
G97-18-2	B	9_6	1358	10434	1.4	4.0	0.3	666	15
G97-18-2	B	9_7	1359	13562	0.9	3.1	0.3	647	15
G97-18-2	B	9_8	1360	15746	2.0	2.6	0.3	636	17
G97-18-2	B	9_9	1361	14518	1.9	2.9	0.3	642	17
G97-18-2	B	9_10	1362	14300	1.3	2.9	0.3	643	16
G97-18-2	B	9_11	1363	9087	1.7	4.6	0.3	677	15
G97-18-2	B	9_12	1364	4108	3.3	10.1	0.9	742	21
G97-18-2	B	9_13	1365	404	32.4	102.8	119.8	998	371
G97-18-2	B	10_1	1367	5153	0.1	8.1	0.5	722	14
G97-18-2	B	10_2	1368	4585	1.4	9.1	0.6	732	16
G97-18-2	B	10_3	1369	5186	1.7	8.0	0.6	722	16
G97-18-2	B	10_4	1370	5705	1.2	7.3	0.5	714	15
G97-18-2	B	10_5	1371	6354	1.0	6.5	0.4	705	14
G97-18-2	B	10_6	1372	2815	0.7	14.8	0.9	776	16
G97-18-2	B	10_7	1373	4969	1.7	8.4	0.6	725	16
G97-18-2	B	10_8	1374	14393	2.0	2.9	0.3	642	17
G97-18-2	B	10_9	1375	13647	1.3	3.0	0.3	646	16
G97-18-2	B	10_10	1376	15192	0.4	2.7	0.2	638	16
G97-18-2	B	10_11	1377	16569	1.4	2.5	0.2	632	17
G97-18-2	B	10_12	1378	13047	2.3	3.2	0.3	649	17
G97-18-2	B	10_13	1379	3394	6.7	12.2	1.9	759	34
G97-18-2	B	10_14	1380	414	9.4	100.4	34.5	994	109
G97-18-2	B	11_1	1381	7254	1.1	5.7	0.4	694	14
G97-18-2	B	11_2	1382	5288	1.1	7.9	0.5	720	15
G97-18-2	B	11_3	1383	4262	0.5	9.7	0.6	739	15
G97-18-2	B	11_4	1384	5539	0.7	7.5	0.5	716	14
G97-18-2	B	11_5	1385	2126	9.4	19.5	4.4	803	52
G97-18-2	B	11_6	1386	3703	1.5	11.2	0.8	751	16
G97-18-2	B	11_7	1387	8276	0.7	5.0	0.3	684	14
G97-18-2	B	11_8	1388	15434	1.5	2.7	0.2	637	16
G97-18-2	B	11_9	1389	14317	1.4	2.9	0.3	643	16
G97-18-2	B	11_10	1390	16413	2.3	2.5	0.3	633	18
G97-18-2	B	11_11	1391	15391	1.3	2.7	0.2	638	16
G97-18-2	B	11_12	1392	17142	2.0	2.4	0.2	630	18
G97-18-2	B	11_13	1393	8423	1.8	4.9	0.4	682	15
G97-18-2	B	11_14	1394	1649	4.9	25.2	3.3	829	33
G97-18-2	B	11_15	1395	158	1.1	263.3	23.3	1142	38
G97-18-2	B	12_1	1396	10216	2.8	4.1	0.4	668	17
G97-18-2	B	12_2	1397	8522	0.6	4.9	0.3	681	14
G97-18-2	B	12_3	1398	5824	0.5	7.1	0.4	712	14

G97-18-2	B	12_4	1399	4783	1.6	8.7	0.6	729	16
G97-18-2	B	12_5	1400	3946	0.7	10.5	0.6	745	15
G97-18-2	B	12_6	1401	5168	1.5	8.0	0.5	722	15
G97-18-2	B	12_7	1402	11793	1.2	3.5	0.3	657	15
G97-18-2	B	12_8	1403	16446	2.7	2.5	0.3	633	18
G97-18-2	B	12_9	1404	16482	0.5	2.5	0.2	633	16
G97-18-2	B	12_10	1405	18479	1.5	2.3	0.2	625	18
G97-18-2	B	12_11	1406	18738	2.2	2.2	0.2	624	18
G97-18-2	B	12_12	1407	19944	2.8	2.1	0.2	620	20
G97-18-2	B	12_13	1408	10100	3.1	4.1	0.4	668	18
G97-18-2	B	12_14	1409	2678	1.1	15.5	1.0	781	17
G97-18-2	B	12_15	1410	394	1.1	105.5	7.5	1001	26
G97-18-2	B	13_1	1411	10977	0.3	3.8	0.3	662	14
G97-18-2	B	13_2	1412	10283	1.6	4.0	0.3	667	15
G97-18-2	B	13_3	1413	8943	0.9	4.6	0.3	678	14
G97-18-2	B	13_4	1414	5832	0.7	7.1	0.4	712	14
G97-18-2	B	13_5	1415	5186	1.2	8.0	0.5	722	15
G97-18-2	B	13_6	1416	8322	1.0	5.0	0.3	683	14
G97-18-2	B	13_7	1417	12327	1.5	3.4	0.3	654	15
G97-18-2	B	13_8	1418	14163	4.1	2.9	0.3	643	21
G97-18-2	B	13_9	1419	16576	1.1	2.5	0.2	632	17
G97-18-2	B	13_10	1420	19364	2.0	2.1	0.2	622	18
G97-18-2	B	13_11	1421	18612	1.3	2.2	0.2	624	17
G97-18-2	B	13_12	1422	18206	0.5	2.3	0.2	626	17
G97-18-2	B	13_13	1423	10134	5.5	4.1	0.5	668	24
G97-18-2	B	13_14	1424	2066	2.7	20.1	1.7	806	22
G97-18-2	B	14_1	1426	10228	2.2	4.1	0.3	667	16
G97-18-2	B	14_2	1427	9740	0.7	4.3	0.3	671	14
G97-18-2	B	14_3	1428	11228	0.4	3.7	0.3	660	14
G97-18-2	B	14_4	1429	12157	1.2	3.4	0.3	655	15
G97-18-2	B	14_5	1430	10652	3.3	3.9	0.4	664	18
G97-18-2	B	14_6	1431	11004	0.5	3.8	0.3	662	14
G97-18-2	B	14_7	1432	14385	2.0	2.9	0.3	642	17
G97-18-2	B	14_8	1433	20677	2.8	2.0	0.2	617	20
G97-18-2	B	14_9	1434	16673	1.6	2.5	0.2	632	17
G97-18-2	B	14_10	1435	9852	4.8	4.2	0.5	670	22
G97-18-2	B	14_11	1436	12077	1.9	3.4	0.3	655	16
G97-18-2	B	14_12	1437	17023	2.0	2.4	0.2	630	18
G97-18-2	B	14_13	1438	10816	2.1	3.8	0.3	663	16
G97-18-2	B	14_14	1439	3840	2.2	10.8	0.8	748	18
G97-18-2	B	14_15	1440	316	1.4	131.3	10.9	1032	31
G97-18-2	B	15_1	1441	10760	2.9	3.9	0.4	664	18
G97-18-2	B	15_2	1442	10640	2.4	3.9	0.3	665	17
G97-18-2	B	15_3	1443	11598	1.1	3.6	0.3	658	15
G97-18-2	B	15_4	1444	12413	0.7	3.4	0.3	653	15
G97-18-2	B	15_5	1445	12519	1.8	3.3	0.3	652	16

G97-18-2	B	15_6	1446	11377	0.8	3.7	0.3	659	15
G97-18-2	B	15_7	1447	11993	1.4	3.5	0.3	656	15
G97-18-2	B	15_8	1448	14491	0.3	2.9	0.2	642	15
G97-18-2	B	15_9	1449	6227	18.7	6.7	2.7	707	76
G97-18-2	B	15_10	1450	13489	2.6	3.1	0.3	647	17
G97-18-2	B	15_11	1451	13395	1.8	3.1	0.3	648	16
G97-18-2	B	15_12	1452	15965	1.9	2.6	0.3	635	17
G97-18-2	B	15_13	1453	11693	1.9	3.6	0.3	657	16
G97-18-2	B	15_14	1454	4447	1.5	9.3	0.6	735	16
G97-18-2	B	15_15	1455	2073	3.8	20.0	2.1	806	26
G97-18-2	B	16_1	1456	15788	1.7	2.6	0.2	636	17
G97-18-2	B	16_2	1457	15284	1.7	2.7	0.3	638	17
G97-18-2	B	16_3	1458	13730	2.2	3.0	0.3	646	17
G97-18-2	B	16_4	1459	14000	1.0	3.0	0.2	644	16
G97-18-2	B	16_5	1460	14401	2.1	2.9	0.3	642	17
G97-18-2	B	16_6	1461	12917	2.3	3.2	0.3	650	17
G97-18-2	B	16_7	1462	14219	1.4	2.9	0.3	643	16
G97-18-2	B	16_8	1463	15495	1.4	2.7	0.2	637	16
G97-18-2	B	16_9	1464	15623	2.2	2.7	0.3	637	17
G97-18-2	B	16_10	1465	14661	3.4	2.8	0.3	641	19
G97-18-2	B	16_11	1466	11860	3.3	3.5	0.4	656	19
G97-18-2	B	16_12	1467	13845	3.1	3.0	0.3	645	18
G97-18-2	B	16_13	1468	9018	2.2	4.6	0.4	677	16
G97-18-2	B	16_14	1469	3816	3.8	10.9	1.1	748	23
G97-18-2	B	16_15	1470	1260	4.0	33.0	3.9	858	32
G97-18-2	B	17_1	1471	16574	6.2	2.5	0.4	632	26
G97-18-2	B	17_2	1472	6628	3.2	6.3	0.6	701	19
G97-18-2	B	17_3	1473	5418	1.4	7.7	0.5	718	15
G97-18-2	B	17_4	1474	9196	0.6	4.5	0.3	676	14
G97-18-2	B	17_5	1475	14759	0.6	2.8	0.2	641	16
G97-18-2	B	17_6	1476	14000	2.9	3.0	0.3	644	18
G97-18-2	B	17_7	1477	14216	1.0	2.9	0.2	643	16
G97-18-2	B	17_8	1478	15310	0.4	2.7	0.2	638	16
G97-18-2	B	17_9	1479	15411	1.3	2.7	0.2	637	16
G97-18-2	B	17_10	1480	16796	2.0	2.5	0.2	631	18
G97-18-2	B	17_11	1481	15808	2.7	2.6	0.3	636	18
G97-18-2	B	17_12	1482	8752	2.2	4.7	0.4	679	16
G97-18-2	B	17_13	1483	4375	3.5	9.5	0.9	736	21
G97-18-2	B	17_14	1484	1188	2.5	34.9	3.1	864	25
G97-18-2	B	17_15	1485	112	2.0	370.3	67.8	1203	80
G97-18-2	B	18_3	1486	1930	2.0	21.5	1.6	813	20
G97-18-2	B	18_4	1487	7328	1.5	5.7	0.4	693	15
G97-18-2	B	18_5	1488	10819	0.6	3.8	0.3	663	14
G97-18-2	B	18_6	1489	11717	2.3	3.5	0.3	657	17
G97-18-2	B	18_7	1490	14020	0.7	3.0	0.2	644	15
G97-18-2	B	18_8	1491	15591	2.8	2.7	0.3	637	18

G97-18-2	B	18_9	1492	7785	5.5	5.3	0.7	689	25
G97-18-2	B	18_10	1493	2681	5.8	15.5	2.3	781	33
G97-18-2	B	18_11	1494	6403	1.9	6.5	0.5	704	16
G97-18-2	B	18_12	1495	6538	2.8	6.4	0.5	703	18
G97-18-2	B	18_13	1496	2214	5.2	18.8	2.6	799	32
G97-18-2	B	18_14	1497	307	3.2	135.1	21.3	1036	55
G97-18-2	B	19_4	1498	3149	6.2	13.2	2.0	766	33
G97-18-2	B	19_5	1499	5429	0.9	7.7	0.5	718	14
G97-18-2	B	19_6	1500	7176	0.8	5.8	0.4	695	14
G97-18-2	B	19_7	1501	9180	2.0	4.5	0.4	676	16
G97-18-2	B	19_8	1502	4370	3.4	9.5	0.9	737	21
G97-18-2	B	19_9	1503	4951	4.8	8.4	1.0	726	25
G97-18-2	B	19_10	1504	6215	4.4	6.7	0.7	707	22
G97-18-2	B	19_11	1505	7310	1.9	5.7	0.4	694	15
G97-18-2	B	19_12	1506	2949	2.5	14.1	1.2	772	20
G97-18-2	B	19_13	1507	795	6.8	52.2	11.0	911	59
G97-18-2	B	20_6	1508	2492	4.3	16.7	1.9	788	27
G97-18-2	B	20_7	1509	4684	2.1	8.9	0.7	730	17
G97-18-2	B	20_8	1510	3448	7.5	12.0	2.1	758	38
G97-18-2	B	20_9	1511	3461	4.2	12.0	1.3	757	25
G97-18-2	B	20_10	1512	6726	1.7	6.2	0.4	700	15
G97-18-2	B	20_11	1513	4412	4.5	9.4	1.1	736	24
G97-18-2	B	20_12	1514	1318	3.6	31.5	3.5	853	30
G97-18-11	A	1_18	470	978	9.5	42.5	7.6	886	49
G97-18-11	A	1_19	471	2922	1.8	14.2	1.0	773	17
G97-18-11	A	1_20	472	3394	6.1	12.2	1.6	759	29
G97-18-11	A	2_15	473	1483	5.6	28.0	3.3	840	31
G97-18-11	A	2_16	474	1746	17.2	23.8	7.8	823	78
G97-18-11	A	2_17	475	2389	6.1	17.4	2.3	792	31
G97-18-11	A	2_18	476	2362	5.1	17.6	2.0	793	27
G97-18-11	A	2_19	477	4809	0.6	8.6	0.5	728	15
G97-18-11	A	2_20	478	7688	0.7	5.4	0.3	690	14
G97-18-11	A	3_13	479	769	4.0	54.0	4.9	915	28
G97-18-11	A	3_14	480	1927	16.7	21.6	6.9	813	75
G97-18-11	A	3_15	481	3744	1.2	11.1	0.7	750	16
G97-18-11	A	3_16	482	2552	6.8	16.3	2.3	786	33
G97-18-11	A	3_17	483	5267	2.0	7.9	0.6	720	16
G97-18-11	A	3_18	484	6050	2.0	6.9	0.5	709	16
G97-18-11	A	3_19	485	8551	0.4	4.9	0.3	681	14
G97-18-11	A	3_20	486	8550	1.1	4.9	0.3	681	14
G97-18-11	A	4_12	487	1485	6.1	28.0	3.6	840	33
G97-18-11	A	4_13	488	2842	5.0	14.6	1.7	775	26
G97-18-11	A	4_14	489	3548	4.5	11.7	1.2	755	24
G97-18-11	A	4_15	490	4537	6.8	9.2	1.3	733	30
G97-18-11	A	4_16	491	5877	3.6	7.1	0.7	711	19

G97-18-11	A	4_17	492	7886	0.8	5.3	0.3	688	14
G97-18-11	A	4_18	493	8960	1.9	4.6	0.3	678	15
G97-18-11	A	4_19	494	8517	1.1	4.9	0.3	682	14
G97-18-11	A	4_20	495	6648	1.1	6.3	0.4	701	14
G97-18-11	A	5_11	496	2730	3.8	15.2	1.4	779	22
G97-18-11	A	5_12	497	5378	2.4	7.7	0.6	719	17
G97-18-11	A	5_13	498	5887	0.9	7.1	0.4	711	14
G97-18-11	A	5_14	499	6238	1.8	6.7	0.5	706	15
G97-18-11	A	5_15	500	7359	1.7	5.6	0.4	693	15
G97-18-11	A	5_16	501	8023	1.2	5.2	0.3	686	14
G97-18-11	A	5_17	502	8773	2.0	4.7	0.4	679	16
G97-18-11	A	5_18	503	7681	1.8	5.4	0.4	690	15
G97-18-11	A	5_19	504	7389	1.2	5.6	0.4	693	14
G97-18-11	A	5_20	505	6136	1.3	6.8	0.4	708	15
G97-18-11	A	6_10	506	3400	4.0	12.2	1.2	759	22
G97-18-11	A	6_11	507	6206	1.7	6.7	0.5	707	15
G97-18-11	A	6_12	508	7484	2.0	5.6	0.4	692	15
G97-18-11	A	6_13	509	8067	1.0	5.2	0.3	686	14
G97-18-11	A	6_14	510	8435	1.2	4.9	0.3	682	14
G97-18-11	A	6_15	511	8298	3.7	5.0	0.5	684	19
G97-18-11	A	6_16	512	8110	2.2	5.1	0.4	685	16
G97-18-11	A	6_17	513	7500	1.4	5.5	0.4	692	14
G97-18-11	A	6_18	514	6874	1.0	6.0	0.4	699	14
G97-18-11	A	6_19	515	6696	0.9	6.2	0.4	701	14
G97-18-11	A	6_20	516	8168	2.7	5.1	0.4	685	17
G97-18-11	A	7_9	517	1360	27.0	30.5	15.6	850	127
G97-18-11	A	7_10	518	5264	1.5	7.9	0.5	721	15
G97-18-11	A	7_11	519	7276	1.4	5.7	0.4	694	15
G97-18-11	A	7_12	520	9259	1.1	4.5	0.3	675	14
G97-18-11	A	7_13	521	9881	2.4	4.2	0.3	670	16
G97-18-11	A	7_14	522	8538	1.3	4.9	0.3	681	14
G97-18-11	A	7_15	523	7945	0.2	5.2	0.3	687	14
G97-18-11	A	7_16	524	7470	1.0	5.6	0.4	692	14
G97-18-11	A	7_17	525	7641	0.7	5.4	0.3	690	14
G97-18-11	A	7_18	526	7112	1.3	5.8	0.4	696	14
G97-18-11	A	7_19	527	7284	1.0	5.7	0.4	694	14
G97-18-11	A	7_20	528	8311	1.0	5.0	0.3	683	14
G97-18-11	A	8_8	529	1648	10.8	25.2	5.4	829	52
G97-18-11	A	8_9	530	4724	4.1	8.8	0.9	730	21
G97-18-11	A	8_10	531	6405	3.8	6.5	0.6	704	20
G97-18-11	A	8_11	532	8561	1.9	4.9	0.4	681	15
G97-18-11	A	8_12	533	9435	1.8	4.4	0.3	674	15
G97-18-11	A	8_13	534	8204	1.1	5.1	0.3	684	14
G97-18-11	A	8_14	535	7422	1.1	5.6	0.4	692	14
G97-18-11	A	8_15	536	6975	0.9	6.0	0.4	697	14
G97-18-11	A	8_16	537	6471	2.8	6.4	0.5	703	17

G97-18-11	A	8_17	538	6541	1.2	6.4	0.4	703	14
G97-18-11	A	8_18	539	6506	0.8	6.4	0.4	703	14
G97-18-11	A	8_19	540	6556	0.7	6.3	0.4	702	14
G97-18-11	A	8_20	541	6620	0.7	6.3	0.4	702	14
G97-18-11	A	9_7	542	2764	5.7	15.0	1.9	778	29
G97-18-11	A	9_8	543	5110	0.4	8.1	0.5	723	14
G97-18-11	A	9_9	544	7296	1.8	5.7	0.4	694	15
G97-18-11	A	9_10	545	9965	1.4	4.2	0.3	669	15
G97-18-11	A	9_11	546	10140	1.8	4.1	0.3	668	15
G97-18-11	A	9_12	547	8382	2.2	5.0	0.4	683	16
G97-18-11	A	9_13	548	7784	1.1	5.3	0.3	689	14
G97-18-11	A	9_14	549	7282	1.3	5.7	0.4	694	14
G97-18-11	A	9_15	550	7128	1.2	5.8	0.4	696	14
G97-18-11	A	9_16	551	7027	1.3	5.9	0.4	697	14
G97-18-11	A	9_17	552	7028	1.7	5.9	0.4	697	15
G97-18-11	A	9_18	553	6940	2.4	6.0	0.5	698	16
G97-18-11	A	9_19	554	7697	0.5	5.4	0.3	689	14
G97-18-11	A	9_20	555	7123	1.9	5.8	0.4	696	15
G97-18-11	A	10_6	556	2856	6.3	14.5	2.0	775	31
G97-18-11	A	10_7	557	4782	1.6	8.7	0.6	729	16
G97-18-11	A	10_8	558	6401	0.5	6.5	0.4	704	14
G97-18-11	A	10_9	559	8870	1.2	4.7	0.3	678	14
G97-18-11	A	10_10	560	9227	1.3	4.5	0.3	675	15
G97-18-11	A	10_11	561	9282	1.1	4.5	0.3	675	14
G97-18-11	A	10_12	562	8746	1.1	4.8	0.3	679	14
G97-18-11	A	10_13	563	7715	2.0	5.4	0.4	689	15
G97-18-11	A	10_14	564	7557	0.4	5.5	0.3	691	14
G97-18-11	A	10_15	565	7821	1.0	5.3	0.3	688	14
G97-18-11	A	10_16	566	7713	1.3	5.4	0.4	689	14
G97-18-11	A	10_17	567	7949	1.5	5.2	0.4	687	15
G97-18-11	A	10_18	568	8515	1.3	4.9	0.3	682	14
G97-18-11	A	10_19	569	8495	0.8	4.9	0.3	682	14
G97-18-11	A	10_20	570	8591	1.9	4.8	0.4	681	15
G97-18-11	A	11_6	571	2683	7.9	15.5	2.5	781	37
G97-18-11	A	11_7	572	5148	2.9	8.1	0.7	722	18
G97-18-11	A	11_8	573	8110	2.1	5.1	0.4	685	16
G97-18-11	A	11_9	574	9182	0.9	4.5	0.3	676	14
G97-18-11	A	11_10	575	7689	0.9	5.4	0.3	690	14
G97-18-11	A	11_11	576	7587	0.7	5.5	0.3	691	14
G97-18-11	A	11_12	577	6766	0.4	6.1	0.4	700	14
G97-18-11	A	11_13	578	6703	3.3	6.2	0.5	701	18
G97-18-11	A	11_14	579	7824	1.4	5.3	0.4	688	15
G97-18-11	A	11_15	580	8293	2.3	5.0	0.4	684	16
G97-18-11	A	11_16	581	8768	0.7	4.7	0.3	679	14
G97-18-11	A	11_17	582	8922	1.4	4.7	0.3	678	15
G97-18-11	A	11_18	583	8699	0.7	4.8	0.3	680	14

G97-18-11	A	11_19	584	8678	2.7	4.8	0.4	680	17
G97-18-11	A	11_20	585	8931	2.1	4.7	0.4	678	16
G97-18-11	A	12_5	586	533	8.7	77.9	13.0	960	51
G97-18-11	A	12_6	587	2874	9.0	14.5	2.7	774	41
G97-18-11	A	12_7	588	6602	1.8	6.3	0.4	702	15
G97-18-11	A	12_8	589	9404	1.1	4.4	0.3	674	14
G97-18-11	A	12_9	590	8400	0.4	4.9	0.3	683	14
G97-18-11	A	12_10	591	7099	2.9	5.9	0.5	696	17
G97-18-11	A	12_11	592	6543	1.8	6.4	0.4	703	15
G97-18-11	A	12_12	593	6556	1.3	6.3	0.4	702	14
G97-18-11	A	12_13	594	6804	0.5	6.1	0.4	699	14
G97-18-11	A	12_14	595	7277	1.0	5.7	0.4	694	14
G97-18-11	A	12_15	596	7999	2.1	5.2	0.4	686	16
G97-18-11	A	12_16	597	8329	0.3	5.0	0.3	683	14
G97-18-11	A	12_17	598	8339	1.8	5.0	0.4	683	15
G97-18-11	A	12_18	599	8138	1.1	5.1	0.3	685	14
G97-18-11	A	12_19	600	7294	2.0	5.7	0.4	694	15
G97-18-11	A	12_20	601	6735	2.2	6.2	0.5	700	16
G97-18-11	A	13_5	602	1557	12.0	26.7	6.4	835	59
G97-18-11	A	13_6	603	3087	8.3	13.5	2.4	768	38
G97-18-11	A	13_7	604	7991	1.5	5.2	0.4	687	15
G97-18-11	A	13_8	605	9677	0.9	4.3	0.3	672	14
G97-18-11	A	13_9	606	8751	0.7	4.8	0.3	679	14
G97-18-11	A	13_10	607	7353	1.6	5.7	0.4	693	15
G97-18-11	A	13_11	608	6837	1.8	6.1	0.4	699	15
G97-18-11	A	13_12	609	7450	0.5	5.6	0.3	692	14
G97-18-11	A	13_13	610	7799	0.8	5.3	0.3	688	14
G97-18-11	A	13_14	611	8718	1.8	4.8	0.4	680	15
G97-18-11	A	13_15	612	8958	1.6	4.6	0.3	678	15
G97-18-11	A	13_16	613	8910	0.9	4.7	0.3	678	14
G97-18-11	A	13_17	614	8561	2.0	4.9	0.4	681	16
G97-18-11	A	13_18	615	8614	1.8	4.8	0.4	681	15
G97-18-11	A	13_19	616	8346	2.1	5.0	0.4	683	16
G97-18-11	A	13_20	617	7616	0.8	5.5	0.3	690	14
G97-18-11	A	14_5	618	2739	2.1	15.2	1.1	779	18
G97-18-11	A	14_6	619	5185	1.1	8.0	0.5	722	15
G97-18-11	A	14_7	620	8501	2.9	4.9	0.4	682	17
G97-18-11	A	14_8	621	8044	2.7	5.2	0.4	686	17
G97-18-11	A	14_9	622	6761	1.2	6.1	0.4	700	14
G97-18-11	A	14_10	623	5760	1.5	7.2	0.5	713	15
G97-18-11	A	14_11	624	5953	1.9	7.0	0.5	710	16
G97-18-11	A	14_12	625	6962	1.9	6.0	0.4	698	15
G97-18-11	A	14_13	626	7642	1.4	5.4	0.4	690	15
G97-18-11	A	14_14	627	7446	1.6	5.6	0.4	692	15
G97-18-11	A	14_15	628	7954	2.2	5.2	0.4	687	16
G97-18-11	A	14_16	629	8062	1.1	5.2	0.3	686	14

G97-18-11	A	14_17	630	7912	1.5	5.3	0.4	687	15
G97-18-11	A	14_18	631	7476	1.9	5.6	0.4	692	15
G97-18-11	A	14_19	632	7516	1.6	5.5	0.4	691	15
G97-18-11	A	14_20	633	7499	1.1	5.5	0.4	692	14
G97-18-11	A	15_4	634	336	8.1	123.5	19.7	1023	54
G97-18-11	A	15_5	635	2165	4.2	19.2	1.9	802	25
G97-18-11	A	15_6	636	6671	0.9	6.2	0.4	701	14
G97-18-11	A	15_7	637	9030	0.9	4.6	0.3	677	14
G97-18-11	A	15_8	638	7639	1.2	5.4	0.4	690	14
G97-18-11	A	15_9	639	6174	1.8	6.7	0.5	707	15
G97-18-11	A	15_10	640	5183	1.7	8.0	0.5	722	16
G97-18-11	A	15_11	641	5867	3.6	7.1	0.7	711	19
G97-18-11	A	15_12	642	7710	2.4	5.4	0.4	689	16
G97-18-11	A	15_13	643	8247	1.5	5.0	0.4	684	15
G97-18-11	A	15_14	644	7862	0.7	5.3	0.3	688	14
G97-18-11	A	15_15	645	7764	1.6	5.4	0.4	689	15
G97-18-11	A	15_16	646	7937	2.7	5.2	0.4	687	17
G97-18-11	A	15_17	647	8061	0.8	5.2	0.3	686	14
G97-18-11	A	15_18	648	7584	2.5	5.5	0.4	691	16
G97-18-11	A	15_19	649	7833	1.7	5.3	0.4	688	15
G97-18-11	A	15_20	650	8371	1.2	5.0	0.3	683	14
G97-18-11	A	16_4	651	3632	5.7	11.4	1.5	753	28
G97-18-11	A	16_5	652	6869	2.5	6.1	0.5	699	16
G97-18-11	A	16_6	653	9485	1.1	4.4	0.3	673	14
G97-18-11	A	16_7	654	9631	0.9	4.3	0.3	672	14
G97-18-11	A	16_8	655	8412	0.7	4.9	0.3	682	14
G97-18-11	A	16_9	656	6491	1.2	6.4	0.4	703	14
G97-18-11	A	16_10	657	5678	1.2	7.3	0.5	714	15
G97-18-11	A	16_11	658	6850	0.3	6.1	0.4	699	14
G97-18-11	A	16_12	659	8814	1.2	4.7	0.3	679	14
G97-18-11	A	16_13	660	9318	2.3	4.5	0.4	675	16
G97-18-11	A	16_14	661	8281	0.6	5.0	0.3	684	14
G97-18-11	A	16_15	662	7838	1.6	5.3	0.4	688	15
G97-18-11	A	16_16	663	8229	1.6	5.1	0.4	684	15
G97-18-11	A	16_17	664	8072	2.1	5.1	0.4	686	16
G97-18-11	A	16_18	665	7755	0.9	5.4	0.3	689	14
G97-18-11	A	16_19	666	8085	1.2	5.1	0.3	686	14
G97-18-11	A	16_20	667	8847	2.6	4.7	0.4	679	17
G97-18-11	A	17_3	668	217	8.8	191.0	33.6	1089	66
G97-18-11	A	17_4	669	3675	2.7	11.3	0.9	752	19
G97-18-11	A	17_5	670	8787	3.1	4.7	0.4	679	18
G97-18-11	A	17_6	671	10391	1.4	4.0	0.3	666	15
G97-18-11	A	17_7	672	8975	0.9	4.6	0.3	677	14
G97-18-11	A	17_8	673	7510	0.9	5.5	0.4	691	14
G97-18-11	A	17_9	674	5723	1.0	7.3	0.5	714	14
G97-18-11	A	17_10	675	6030	1.6	6.9	0.5	709	15

G97-18-11	A	17_11	676	6922	0.7	6.0	0.4	698	14
G97-18-11	A	17_12	677	8430	1.8	4.9	0.4	682	15
G97-18-11	A	17_13	678	6916	2.2	6.0	0.4	698	16
G97-18-11	A	17_14	679	8898	1.7	4.7	0.3	678	15
G97-18-11	A	17_15	680	8180	1.1	5.1	0.3	685	14
G97-18-11	A	17_16	681	8345	1.7	5.0	0.4	683	15
G97-18-11	A	17_17	682	8259	0.9	5.0	0.3	684	14
G97-18-11	A	17_18	683	8601	2.0	4.8	0.4	681	16
G97-18-11	A	17_19	684	8996	0.7	4.6	0.3	677	14
G97-18-11	A	17_20	685	9630	3.4	4.3	0.4	672	18
G97-18-11	A	18_2	686	92	39.3	453.2	337.9	1242	337
G97-18-11	A	18_3	687	162	33.1	256.9	165.8	1138	253
G97-18-11	A	18_4	688	2100	0.3	19.8	1.2	805	16
G97-18-11	A	18_5	689	8511	2.0	4.9	0.4	682	16
G97-18-11	A	18_6	690	8589	1.3	4.8	0.3	681	14
G97-18-11	A	18_7	691	8099	1.4	5.1	0.4	685	15
G97-18-11	A	18_8	692	7425	2.0	5.6	0.4	692	15
G97-18-11	A	18_9	693	5853	0.8	7.1	0.4	712	14
G97-18-11	A	18_10	694	3162	2.5	13.1	1.0	766	19
G97-18-11	A	18_11	695	3775	1.3	11.0	0.7	749	16
G97-18-11	A	18_12	696	6956	0.4	6.0	0.4	698	14
G97-18-11	A	18_13	697	7497	0.8	5.5	0.3	692	14
G97-18-11	A	18_14	698	8483	1.5	4.9	0.3	682	15
G97-18-11	A	18_15	699	8833	1.2	4.7	0.3	679	14
G97-18-11	A	18_16	700	9213	1.1	4.5	0.3	675	14
G97-18-11	A	18_17	701	8896	1.9	4.7	0.4	678	15
G97-18-11	A	18_18	702	9323	1.5	4.5	0.3	675	15
G97-18-11	A	18_19	703	10256	0.6	4.1	0.3	667	14
G97-18-11	A	18_20	704	8536	3.1	4.9	0.4	681	18
G97-18-11	A	19_2	705	857	0.2	48.5	2.8	902	19
G97-18-11	A	19_3	706	1121	3.2	37.1	3.2	871	25
G97-18-11	A	19_4	707	3514	4.1	11.8	1.2	756	23
G97-18-11	A	19_5	708	9111	3.3	4.6	0.4	676	18
G97-18-11	A	19_6	709	7753	0.4	5.4	0.3	689	14
G97-18-11	A	19_7	710	7111	1.3	5.8	0.4	696	14
G97-18-11	A	19_8	711	6631	0.9	6.3	0.4	701	14
G97-18-11	A	19_9	712	1473	1.0	28.2	1.7	841	18
G97-18-11	A	19_10	713	180	0.6	230.6	13.8	1120	27
G97-18-11	A	19_11	714	249	0.5	166.7	9.9	1068	25
G97-18-11	A	19_12	715	3711	0.7	11.2	0.7	751	15
G97-18-11	A	19_13	716	6918	1.2	6.0	0.4	698	14
G97-18-11	A	19_14	717	7770	1.8	5.3	0.4	689	15
G97-18-11	A	19_15	718	9138	1.2	4.5	0.3	676	14
G97-18-11	A	19_16	719	9657	1.1	4.3	0.3	672	14
G97-18-11	A	19_17	720	9970	2.5	4.2	0.4	669	16
G97-18-11	A	19_18	721	10718	1.2	3.9	0.3	664	15

G97-18-11	A	19_19	722	10121	2.4	4.1	0.3	668	16
G97-18-11	A	19_20	723	749	3.2	55.4	4.9	918	27
G97-18-11	A	20_1	724	4151	3.9	10.0	1.0	741	22
G97-18-11	A	20_2	725	6209	3.5	6.7	0.6	707	19
G97-18-11	A	20_3	726	6526	1.8	6.4	0.4	703	15
G97-18-11	A	20_4	727	9334	0.7	4.5	0.3	674	14
G97-18-11	A	20_5	728	9769	2.6	4.3	0.4	671	17
G97-18-11	A	20_6	729	8377	2.3	5.0	0.4	683	16
G97-18-11	A	20_7	730	7436	1.6	5.6	0.4	692	15
G97-18-11	A	20_8	731	4425	1.4	9.4	0.6	735	16
G97-18-11	A	20_9	732	51	2.2	809.5	66.8	1365	47
G97-18-11	A	20_12	735	121	0.8	343.7	21.1	1189	30
G97-18-11	A	20_13	736	6152	1.5	6.8	0.4	708	15
G97-18-11	A	20_14	737	8094	2.5	5.1	0.4	686	16
G97-18-11	A	20_15	738	9350	1.8	4.4	0.3	674	15
G97-18-11	A	20_16	739	10319	1.8	4.0	0.3	667	15
G97-18-11	A	20_17	740	12525	1.3	3.3	0.3	652	15
G97-18-11	A	20_18	741	10776	2.3	3.9	0.3	664	16
G97-18-11	A	20_19	742	2414	4.4	17.2	1.8	791	25
G97-18-11	A	20_20	743	586	4.5	70.8	7.8	948	34
G97-18-11	A	21_1	744	5400	2.0	7.7	0.5	718	16
G97-18-11	A	21_2	745	9481	3.3	4.4	0.4	673	18
G97-18-11	A	21_3	746	9902	1.7	4.2	0.3	670	15
G97-18-11	A	21_4	747	11459	0.5	3.6	0.3	659	14
G97-18-11	A	21_5	748	10757	1.4	3.9	0.3	664	15
G97-18-11	A	21_6	749	9494	1.0	4.4	0.3	673	14
G97-18-11	A	21_7	750	9170	1.1	4.5	0.3	676	14
G97-18-11	A	21_8	751	4866	1.3	8.5	0.5	727	15
G97-18-11	A	21_9	752	18	0.6	2350.6	154.1	1652	54
G97-18-11	A	21_12	755	31	0.8	1333.9	86.9	1488	45
G97-18-11	A	21_13	756	4404	1.2	9.4	0.6	736	15
G97-18-11	A	21_14	757	8908	2.3	4.7	0.4	678	16
G97-18-11	A	21_15	758	9394	1.2	4.4	0.3	674	14
G97-18-11	A	21_16	759	5727	7.7	7.3	1.2	713	33
G97-18-11	A	21_17	760	6002	4.2	6.9	0.7	710	21
G97-18-11	A	21_18	761	536	3.0	77.5	6.7	960	28
G97-18-11	A	21_19	762	361	1.2	114.9	7.3	1013	24
G97-18-11	A	21_20	763	202	3.7	205.1	21.2	1101	41
G97-18-11	A	22_1	764	9284	8.5	4.5	0.8	675	33
G97-18-11	A	22_2	765	12285	2.6	3.4	0.3	654	17
G97-18-11	A	22_3	766	13849	1.0	3.0	0.3	645	15
G97-18-11	A	22_4	767	15466	2.0	2.7	0.3	637	17
G97-18-11	A	22_5	768	12639	2.0	3.3	0.3	652	16
G97-18-11	A	22_6	769	9874	1.2	4.2	0.3	670	15
G97-18-11	A	22_7	770	9510	0.6	4.4	0.3	673	14
G97-18-11	A	22_8	771	9079	1.3	4.6	0.3	677	15

G97-18-11	A	22_9	772	7551	1.1	5.5	0.4	691	14
G97-18-11	A	22_10	773	683	0.6	60.8	3.6	929	20
G97-18-11	A	22_11	774	953	0.6	43.6	2.6	889	19
G97-18-11	A	22_12	775	7602	1.5	5.5	0.4	690	15
G97-18-11	A	22_13	776	10240	2.3	4.1	0.3	667	16
G97-18-11	A	22_14	777	12261	3.7	3.4	0.4	654	19
G97-18-11	A	22_15	778	9660	2.9	4.3	0.4	672	17
G97-18-11	A	22_16	779	5058	2.4	8.2	0.6	724	17
G97-18-11	A	22_17	780	1141	2.1	36.4	2.6	869	21
G97-18-11	A	22_18	781	157	1.7	265.3	19.0	1144	32
G97-18-11	A	22_19	782	5	1.5	8898.2	2702.2	2192	365
G97-18-11	A	23_1	783	10571	6.4	3.9	0.6	665	27
G97-18-11	A	23_2	784	17625	2.2	2.4	0.2	628	18
G97-18-11	A	23_3	785	21075	1.4	2.0	0.2	616	19
G97-18-11	A	23_4	786	17178	2.9	2.4	0.3	630	19
G97-18-11	A	23_5	787	11614	1.6	3.6	0.3	658	15
G97-18-11	A	23_6	788	8260	0.9	5.0	0.3	684	14
G97-18-11	A	23_7	789	7469	1.4	5.6	0.4	692	14
G97-18-11	A	23_8	790	8526	1.5	4.9	0.3	681	15
G97-18-11	A	23_9	791	9303	0.5	4.5	0.3	675	14
G97-18-11	A	23_10	792	10913	2.5	3.8	0.3	663	17
G97-18-11	A	23_11	793	11124	1.9	3.7	0.3	661	16
G97-18-11	A	23_12	794	11019	0.4	3.8	0.3	662	14
G97-18-11	A	23_13	795	8992	1.5	4.6	0.3	677	15
G97-18-11	A	23_14	796	3663	2.1	11.3	0.8	752	17
G97-18-11	A	23_15	797	3410	1.5	12.2	0.8	759	16
G97-18-11	A	23_16	798	3069	1.9	13.5	1.0	768	17
G97-18-11	A	23_17	799	1383	2.7	30.0	2.4	848	22
G97-18-11	A	23_18	800	336	1.3	123.7	8.1	1024	25
G97-18-11	A	24_1	801	9473	11.0	4.4	1.0	673	42
G97-18-11	A	24_2	802	13793	1.0	3.0	0.3	645	15
G97-18-11	A	24_3	803	18089	1.4	2.3	0.2	626	17
G97-18-11	A	24_4	804	13853	1.7	3.0	0.3	645	16
G97-18-11	A	24_5	805	9205	2.6	4.5	0.4	676	17
G97-18-11	A	24_6	806	7367	0.8	5.6	0.4	693	14
G97-18-11	A	24_7	807	6891	1.4	6.0	0.4	698	15
G97-18-11	A	24_8	808	8178	1.3	5.1	0.3	685	14
G97-18-11	A	24_9	809	9708	0.9	4.3	0.3	671	14
G97-18-11	A	24_10	810	9798	1.6	4.2	0.3	671	15
G97-18-11	A	24_11	811	8510	0.8	4.9	0.3	682	14
G97-18-11	A	24_12	812	8700	2.2	4.8	0.4	680	16
G97-18-11	A	24_13	813	3191	3.2	13.0	1.1	765	20
G97-18-11	A	24_14	814	2351	5.5	17.7	2.2	794	30
G97-18-11	A	24_15	815	1356	3.1	30.6	2.6	850	24
G97-18-11	A	24_16	816	1262	1.9	32.9	2.3	858	20
G97-18-11	A	25_1	817	5903	8.1	7.0	1.2	711	34

G97-18-11	A	25_2	818	10771	2.2	3.9	0.3	664	16
G97-18-11	A	25_3	819	14231	2.2	2.9	0.3	643	17
G97-18-11	A	25_4	820	10436	1.7	4.0	0.3	666	15
G97-18-11	A	25_5	821	7156	3.2	5.8	0.5	695	18
G97-18-11	A	25_6	822	8772	2.0	4.7	0.4	679	16
G97-18-11	A	25_7	823	9148	2.0	4.5	0.4	676	16
G97-18-11	A	25_8	824	8935	1.9	4.7	0.3	678	15
G97-18-11	A	25_9	825	5245	1.6	7.9	0.5	721	15
G97-18-11	A	25_10	826	6362	1.7	6.5	0.4	705	15
G97-18-11	A	25_11	827	10074	1.9	4.1	0.3	669	16
G97-18-11	A	25_12	828	7074	2.6	5.9	0.5	696	17
G97-18-11	A	25_13	829	4118	5.5	10.1	1.3	742	27
G97-18-11	A	25_14	830	1395	3.3	29.8	2.7	847	25
G97-18-11	A	26_2	831	5135	16.3	8.1	2.7	723	66
G97-18-11	A	26_3	832	763	11.4	54.4	13.9	915	72
G97-18-11	A	26_4	833	1480	17.3	28.1	10.3	841	90
G97-18-11	A	26_5	834	5141	2.0	8.1	0.6	723	16
G97-18-11	A	26_6	835	1383	31.7	30.0	20.0	848	165
G97-18-11	A	26_7	836	2932	0.9	14.2	0.9	773	16
G97-18-11	A	26_8	837	770	2.9	53.9	4.6	914	26
G97-18-11	A	26_9	838	1393	5.0	29.8	3.6	847	31
G97-18-11	A	26_10	839	1898	2.9	21.9	1.8	815	22
G97-18-11	A	26_11	840	3710	4.5	11.2	1.2	751	24
G97-18-11	A	26_12	841	2286	6.3	18.2	2.6	796	33
G97-18-11	B	1_1	842	1837	3.4	22.6	2.1	818	24
G97-18-11	B	1_2	843	1899	1.1	21.9	1.4	815	17
G97-18-11	B	1_3	844	29	9.0	1430.9	890.9	1507	389
G97-18-11	B	1_4	845	495	11.4	83.9	22.5	970	82
G97-18-11	B	1_5	846	768	1.7	54.1	3.8	915	22
G97-18-11	B	1_6	847	2652	1.9	15.7	1.1	782	18
G97-18-11	B	1_7	848	1839	1.3	22.6	1.5	818	18
G97-18-11	B	1_8	849	2076	3.8	20.0	2.0	806	24
G97-18-11	B	1_9	850	2495	0.5	16.6	1.0	788	16
G97-18-11	B	1_10	851	4900	1.7	8.5	0.6	727	16
G97-18-11	B	1_11	852	5479	3.5	7.6	0.7	717	20
G97-18-11	B	1_12	853	4447	5.5	9.3	1.2	735	27
G97-18-11	B	1_13	854	5950	4.2	7.0	0.7	710	21
G97-18-11	B	1_14	855	6614	3.6	6.3	0.6	702	19
G97-18-11	B	1_15	856	2353	4.6	17.7	2.0	793	27
G97-18-11	B	2_1	857	4335	2.5	9.6	0.7	737	18
G97-18-11	B	2_2	858	4008	1.0	10.4	0.6	744	15
G97-18-11	B	2_3	859	2903	1.2	14.3	0.9	773	16
G97-18-11	B	2_4	860	4928	1.0	8.4	0.5	726	15
G97-18-11	B	2_5	861	9618	1.1	4.3	0.3	672	14
G97-18-11	B	2_6	862	8608	1.6	4.8	0.3	681	15
G97-18-11	B	2_7	863	7993	0.8	5.2	0.3	687	14

G97-18-11	B	2_8	864	9099	2.0	4.6	0.4	676	16
G97-18-11	B	2_9	865	8910	1.3	4.7	0.3	678	15
G97-18-11	B	2_10	866	11745	1.2	3.5	0.3	657	15
G97-18-11	B	2_11	867	13311	2.4	3.1	0.3	648	17
G97-18-11	B	2_12	868	14397	2.2	2.9	0.3	642	17
G97-18-11	B	2_13	869	15935	2.5	2.6	0.3	635	18
G97-18-11	B	2_14	870	15672	3.7	2.7	0.3	636	20
G97-18-11	B	2_15	871	7062	3.5	5.9	0.5	696	19
G97-18-11	B	3_1	872	7758	2.7	5.4	0.4	689	17
G97-18-11	B	3_2	873	6559	1.6	6.3	0.4	702	15
G97-18-11	B	3_3	874	5978	0.5	7.0	0.4	710	14
G97-18-11	B	3_4	875	7350	2.0	5.7	0.4	693	15
G97-18-11	B	3_5	876	7889	1.1	5.3	0.3	688	14
G97-18-11	B	3_6	877	6878	0.8	6.0	0.4	698	14
G97-18-11	B	3_7	878	6581	0.7	6.3	0.4	702	14
G97-18-11	B	3_8	879	6792	2.9	6.1	0.5	699	17
G97-18-11	B	3_9	880	7377	1.3	5.6	0.4	693	14
G97-18-11	B	3_10	881	11338	0.6	3.7	0.3	660	14
G97-18-11	B	3_11	882	13984	1.6	3.0	0.3	644	16
G97-18-11	B	3_12	883	14065	1.3	3.0	0.3	644	16
G97-18-11	B	3_13	884	14058	3.3	3.0	0.3	644	19
G97-18-11	B	3_14	885	16369	1.5	2.5	0.2	633	17
G97-18-11	B	3_15	886	8960	4.2	4.6	0.5	678	20
G97-18-11	B	4_1	887	7479	2.2	5.6	0.4	692	16
G97-18-11	B	4_2	888	6551	0.2	6.3	0.4	702	14
G97-18-11	B	4_3	889	6615	1.0	6.3	0.4	702	14
G97-18-11	B	4_4	890	6899	1.3	6.0	0.4	698	14
G97-18-11	B	4_5	891	7308	0.9	5.7	0.4	694	14
G97-18-11	B	4_6	892	7807	1.0	5.3	0.3	688	14
G97-18-11	B	4_7	893	7941	2.2	5.2	0.4	687	16
G97-18-11	B	4_8	894	6651	1.9	6.2	0.4	701	15
G97-18-11	B	4_9	895	6100	2.2	6.8	0.5	708	16
G97-18-11	B	4_10	896	7633	2.8	5.4	0.5	690	17
G97-18-11	B	4_11	897	10095	1.9	4.1	0.3	668	16
G97-18-11	B	4_12	898	12110	2.2	3.4	0.3	655	16
G97-18-11	B	4_13	899	13446	3.0	3.1	0.3	647	18
G97-18-11	B	4_14	900	15365	3.2	2.7	0.3	638	19
G97-18-11	B	4_15	901	9655	2.0	4.3	0.3	672	16
G97-18-11	B	5_1	902	6719	0.9	6.2	0.4	700	14
G97-18-11	B	5_2	903	5649	1.3	7.4	0.5	715	15
G97-18-11	B	5_3	904	5975	0.4	7.0	0.4	710	14
G97-18-11	B	5_4	905	6366	1.4	6.5	0.4	705	15
G97-18-11	B	5_5	906	6428	1.2	6.5	0.4	704	14
G97-18-11	B	5_6	907	6829	1.2	6.1	0.4	699	14
G97-18-11	B	5_7	908	7369	1.7	5.6	0.4	693	15
G97-18-11	B	5_8	909	8249	2.3	5.0	0.4	684	16

G97-18-11	B	5_9	910	8494	1.0	4.9	0.3	682	14
G97-18-11	B	5_10	911	6370	2.1	6.5	0.5	705	16
G97-18-11	B	5_11	912	5981	1.5	6.9	0.5	710	15
G97-18-11	B	5_12	913	8421	1.5	4.9	0.3	682	15
G97-18-11	B	5_13	914	11722	1.2	3.5	0.3	657	15
G97-18-11	B	5_14	915	15291	1.0	2.7	0.2	638	16
G97-18-11	B	5_15	916	10535	2.5	3.9	0.3	665	17
G97-18-11	B	6_1	917	7158	0.8	5.8	0.4	695	14
G97-18-11	B	6_2	918	6853	1.8	6.1	0.4	699	15
G97-18-11	B	6_3	919	7235	1.1	5.7	0.4	694	14
G97-18-11	B	6_4	920	7420	0.9	5.6	0.4	692	14
G97-18-11	B	6_5	921	7378	2.3	5.6	0.4	693	16
G97-18-11	B	6_6	922	7641	1.3	5.4	0.4	690	14
G97-18-11	B	6_7	923	7908	2.1	5.3	0.4	687	16
G97-18-11	B	6_8	924	7006	1.3	5.9	0.4	697	14
G97-18-11	B	6_9	925	8386	0.4	5.0	0.3	683	14
G97-18-11	B	6_10	926	6940	1.3	6.0	0.4	698	14
G97-18-11	B	6_11	927	5233	1.6	7.9	0.5	721	16
G97-18-11	B	6_12	928	7500	0.7	5.5	0.3	692	14
G97-18-11	B	6_13	929	10942	1.7	3.8	0.3	662	15
G97-18-11	B	6_14	930	13026	2.1	3.2	0.3	650	16
G97-18-11	B	6_15	931	3391	3.6	12.2	1.2	759	22
G97-18-11	B	7_1	932	7414	1.6	5.6	0.4	692	15
G97-18-11	B	7_2	933	8305	1.5	5.0	0.4	684	15
G97-18-11	B	7_3	934	8397	1.0	4.9	0.3	683	14
G97-18-11	B	7_4	935	8453	2.5	4.9	0.4	682	16
G97-18-11	B	7_5	936	8987	1.7	4.6	0.3	677	15
G97-18-11	B	7_6	937	9214	1.9	4.5	0.3	675	15
G97-18-11	B	7_7	938	9600	1.5	4.3	0.3	672	15
G97-18-11	B	7_8	939	9415	0.9	4.4	0.3	674	14
G97-18-11	B	7_9	940	5918	0.9	7.0	0.4	711	14
G97-18-11	B	7_10	941	887	10.4	46.8	11.4	898	66
G97-18-11	B	7_11	942	4443	4.3	9.4	1.0	735	23
G97-18-11	B	7_12	943	8673	2.1	4.8	0.4	680	16
G97-18-11	B	7_13	944	11592	1.6	3.6	0.3	658	15
G97-18-11	B	7_14	945	10971	2.3	3.8	0.3	662	16
G97-18-11	B	7_15	946	4526	0.8	9.2	0.6	733	15
G97-18-11	B	8_1	947	7079	1.4	5.9	0.4	696	15
G97-18-11	B	8_2	948	6172	2.0	6.7	0.5	707	16
G97-18-11	B	8_3	949	7326	0.6	5.7	0.4	693	14
G97-18-11	B	8_4	950	8234	1.0	5.0	0.3	684	14
G97-18-11	B	8_5	951	8696	1.9	4.8	0.4	680	15
G97-18-11	B	8_6	952	8936	2.7	4.7	0.4	678	17
G97-18-11	B	8_7	953	9675	0.8	4.3	0.3	672	14
G97-18-11	B	8_8	954	10252	2.1	4.1	0.3	667	16
G97-18-11	B	8_9	955	6905	0.8	6.0	0.4	698	14

G97-18-11	B	8_10	956	2038	1.2	20.4	1.3	808	17
G97-18-11	B	8_11	957	2247	0.4	18.5	1.1	798	16
G97-18-11	B	8_12	958	8097	1.6	5.1	0.4	685	15
G97-18-11	B	8_13	959	11315	2.5	3.7	0.3	660	17
G97-18-11	B	8_14	960	8274	2.7	5.0	0.4	684	17
G97-18-11	B	8_15	961	1555	18.7	26.7	10.9	835	99
G97-18-11	B	9_1	962	7655	2.7	5.4	0.4	690	17
G97-18-11	B	9_2	963	7637	2.4	5.4	0.4	690	16
G97-18-11	B	9_3	964	7610	2.5	5.5	0.4	690	17
G97-18-11	B	9_4	965	7874	0.6	5.3	0.3	688	14
G97-18-11	B	9_5	966	7996	2.1	5.2	0.4	686	16
G97-18-11	B	9_6	967	9103	1.7	4.6	0.3	676	15
G97-18-11	B	9_7	968	10839	1.3	3.8	0.3	663	15
G97-18-11	B	9_8	969	10963	2.5	3.8	0.3	662	17
G97-18-11	B	9_9	970	6869	2.3	6.1	0.5	699	16
G97-18-11	B	9_10	971	1248	0.7	33.3	2.0	859	18
G97-18-11	B	9_11	972	1213	0.7	34.2	2.1	862	18
G97-18-11	B	9_12	973	4692	0.9	8.9	0.5	730	15
G97-18-11	B	9_13	974	6158	3.2	6.7	0.6	707	18
G97-18-11	B	9_14	975	3200	20.9	13.0	5.7	764	94
G97-18-11	B	10_1	977	8779	1.7	4.7	0.3	679	15
G97-18-11	B	10_2	978	9342	2.4	4.4	0.4	674	16
G97-18-11	B	10_3	979	8958	1.8	4.6	0.3	678	15
G97-18-11	B	10_4	980	7738	1.5	5.4	0.4	689	15
G97-18-11	B	10_5	981	8072	1.4	5.1	0.4	686	15
G97-18-11	B	10_6	982	9178	1.4	4.5	0.3	676	15
G97-18-11	B	10_7	983	10391	1.6	4.0	0.3	666	15
G97-18-11	B	10_8	984	9868	3.0	4.2	0.4	670	18
G97-18-11	B	10_9	985	7150	1.0	5.8	0.4	695	14
G97-18-11	B	10_10	986	1556	1.0	26.7	1.7	835	18
G97-18-11	B	10_11	987	1143	0.9	36.3	2.2	869	19
G97-18-11	B	10_12	988	2291	0.7	18.1	1.1	796	16
G97-18-11	B	10_13	989	1434	2.2	29.0	2.2	844	21
G97-18-11	B	10_14	990	393	1.8	105.8	8.0	1002	27
G97-18-11	B	11_1	991	7702	2.2	5.4	0.4	689	16
G97-18-11	B	11_2	992	8843	2.4	4.7	0.4	679	16
G97-18-11	B	11_3	993	9447	1.3	4.4	0.3	674	15
G97-18-11	B	11_4	994	8772	2.1	4.7	0.4	679	16
G97-18-11	B	11_5	995	8113	2.7	5.1	0.4	685	17
G97-18-11	B	11_6	996	8372	0.4	5.0	0.3	683	14
G97-18-11	B	11_7	997	9813	1.0	4.2	0.3	671	14
G97-18-11	B	11_8	998	10278	1.2	4.0	0.3	667	15
G97-18-11	B	11_9	999	8942	1.5	4.6	0.3	678	15
G97-18-11	B	11_10	1000	3039	1.0	13.7	0.9	769	16
G97-18-11	B	11_11	1001	1781	0.8	23.3	1.4	821	17
G97-18-11	B	11_12	1002	1316	0.9	31.6	2.0	853	18

G97-18-11	B	11_13	1003	659	6.1	63.1	10.1	934	47
G97-18-11	B	11_14	1004	141	2.6	295.4	36.4	1162	52
G97-18-11	B	12_1	1005	7005	1.1	5.9	0.4	697	14
G97-18-11	B	12_2	1006	8325	1.1	5.0	0.3	683	14
G97-18-11	B	12_3	1007	8610	1.4	4.8	0.3	681	15
G97-18-11	B	12_4	1008	9018	0.4	4.6	0.3	677	14
G97-18-11	B	12_5	1009	8419	0.4	4.9	0.3	682	14
G97-18-11	B	12_6	1010	9202	1.5	4.5	0.3	676	15
G97-18-11	B	12_7	1011	10259	1.2	4.1	0.3	667	15
G97-18-11	B	12_8	1012	9587	0.5	4.3	0.3	672	14
G97-18-11	B	12_9	1013	9900	1.7	4.2	0.3	670	15
G97-18-11	B	12_10	1014	8334	0.8	5.0	0.3	683	14
G97-18-11	B	12_11	1015	6141	1.7	6.8	0.5	708	15
G97-18-11	B	12_12	1016	1253	14.5	33.2	10.9	859	84
G97-18-11	B	13_1	1018	7065	1.2	5.9	0.4	696	14
G97-18-11	B	13_2	1019	8735	1.3	4.8	0.3	680	15
G97-18-11	B	13_3	1020	9220	2.4	4.5	0.4	675	16
G97-18-11	B	13_4	1021	8469	1.8	4.9	0.4	682	15
G97-18-11	B	13_5	1022	601	1.6	69.0	4.9	945	24
G97-18-11	B	13_6	1023	682	0.8	60.9	3.7	929	21
G97-18-11	B	13_7	1024	4622	1.4	9.0	0.6	732	15
G97-18-11	B	13_8	1025	8177	4.2	5.1	0.5	685	21
G97-18-11	B	13_9	1026	4186	12.9	9.9	2.7	740	56
G97-18-11	B	13_10	1027	99	10.7	419.3	234.2	1227	248
G97-18-11	B	14_1	1030	7318	2.4	5.7	0.4	694	16
G97-18-11	B	14_2	1031	8631	0.4	4.8	0.3	680	14
G97-18-11	B	14_3	1032	6738	1.7	6.2	0.4	700	15
G97-18-11	B	14_4	1033	77	0.4	542.1	34.2	1278	34
G97-18-11	B	14_7	1036	642	0.8	64.7	4.0	937	21
G97-18-11	B	14_8	1037	7204	1.1	5.8	0.4	695	14
G97-18-11	B	14_9	1038	3640	3.3	11.4	1.0	753	21
G97-18-11	B	15_1	1041	8276	1.3	5.0	0.3	684	15
G97-18-11	B	15_2	1042	9077	1.1	4.6	0.3	677	14
G97-18-11	B	15_3	1043	5754	1.6	7.2	0.5	713	15
G97-18-11	B	15_4	1044	157	0.3	263.7	15.8	1142	28
G97-18-11	B	15_7	1047	267	0.4	155.5	9.3	1057	25
G97-18-11	B	15_8	1048	1355	3.9	30.7	3.3	850	28
G97-18-11	B	16_1	1050	9032	0.5	4.6	0.3	677	14
G97-18-11	B	16_2	1051	10092	1.9	4.1	0.3	668	16
G97-18-11	B	16_3	1052	11938	4.6	3.5	0.4	656	22
G97-18-11	B	16_4	1053	9370	1.7	4.4	0.3	674	15
G97-18-11	B	16_5	1054	3328	1.0	12.5	0.8	761	16
G97-18-11	B	16_6	1055	702	9.4	59.2	14.3	926	69
G97-18-11	B	17_1	1058	9582	0.6	4.3	0.3	672	14
G97-18-11	B	17_2	1059	8918	2.8	4.7	0.4	678	17
G97-18-11	B	17_3	1060	9852	1.8	4.2	0.3	670	15

G97-18-11	B	17_4	1061	1921	0.6	21.6	1.3	814	17
G97-18-11	B	17_5	1062	407	27.6	102.1	80.8	997	251
G97-18-11	B	17_6	1063	599	15.3	69.4	27.8	946	118
G97-18-11	B	18_1	1065	1085	0.5	38.3	2.3	875	19
G97-18-11	B	18_2	1066	927	0.4	44.8	2.6	892	19
G97-18-11	B	18_3	1067	582	4.3	71.3	9.1	949	39
G97-18-11	B	18_4	1068	525	2.7	79.1	7.3	962	30
G97-18-11	B	19_1	1070	6	1.4	6893.4	5954.2	2066	931
G97-18-11	B	19_3	1072	109	1.1	381.6	31.9	1209	39
FC1-7	A	1_2	281	2971	1.2	14.0	0.9	771	16
FC1-7	A	1_3	282	1924	2.0	21.6	1.5	813	19
FC1-7	A	1_4	283	381	3.2	108.9	7.2	1006	25
FC1-7	A	1_2	284	3044	0.8	13.6	0.8	769	16
FC1-7	A	1_3	285	2014	1.6	20.6	1.4	809	18
FC1-7	A	1_4	286	479	0.3	86.7	5.1	975	21
FC1-7	A	2_1	287	1069	14.2	38.9	9.3	876	63
FC1-7	A	2_2	288	2587	0.7	16.1	1.0	784	16
FC1-7	A	2_3	289	1893	0.8	21.9	1.3	815	17
FC1-7	A	2_4	290	597	1.1	69.6	4.2	946	21
FC1-7	A	3_1	291	3922	2.1	10.6	0.7	746	17
FC1-7	A	3_2	292	2977	0.7	14.0	0.8	771	16
FC1-7	A	3_3	293	1916	0.5	21.7	1.3	814	17
FC1-7	A	3_4	294	1865	0.9	22.3	1.4	817	17
FC1-7	A	3_5	295	1272	4.4	32.6	3.1	857	26
FC1-7	A	4_1	296	4076	3.1	10.2	0.9	743	19
FC1-7	A	4_2	297	3216	0.6	12.9	0.8	764	15
FC1-7	A	4_3	298	1965	0.5	21.1	1.3	811	17
FC1-7	A	4_4	299	1942	0.6	21.4	1.3	812	17
FC1-7	A	4_5	300	1840	0.2	22.6	1.3	818	17
FC1-7	A	4_6	301	985	3.4	42.2	3.4	885	24
FC1-7	A	5_2	302	3165	0.3	13.1	0.8	765	15
FC1-7	A	5_3	303	2038	0.7	20.4	1.2	808	17
FC1-7	A	5_4	304	1941	0.4	21.4	1.3	813	17
FC1-7	A	5_5	305	1951	0.5	21.3	1.3	812	17
FC1-7	A	5_6	306	1699	2.0	24.4	1.7	826	19
FC1-7	A	6_2	307	3474	1.2	12.0	0.8	757	16
FC1-7	A	6_3	308	2155	0.4	19.3	1.1	802	16
FC1-7	A	6_4	309	1922	0.3	21.6	1.3	814	17
FC1-7	A	6_5	310	2032	0.7	20.4	1.2	808	17
FC1-7	A	6_6	311	570	8.1	72.8	9.0	952	38
FC1-7	A	6_7	312	221	1.2	187.9	11.0	1087	25
FC1-7	A	7_1	313	2537	17.8	16.4	5.5	786	75
FC1-7	A	7_2	314	3546	2.3	11.7	0.9	755	17
FC1-7	A	7_3	315	2238	0.5	18.6	1.1	798	16
FC1-7	A	7_4	316	1961	0.4	21.2	1.3	812	17

FC1-7	A	7_5	317	2086	0.4	19.9	1.2	805	16
FC1-7	A	7_6	318	2003	0.8	20.7	1.3	809	17
FC1-7	A	7_7	319	1371	12.5	30.3	6.8	849	57
FC1-7	A	8_2	320	4288	0.5	9.7	0.6	738	15
FC1-7	A	8_3	321	2360	0.7	17.6	1.1	793	16
FC1-7	A	8_4	322	2005	0.7	20.7	1.2	809	17
FC1-7	A	8_5	323	1935	0.3	21.5	1.3	813	17
FC1-7	A	8_6	324	2154	0.4	19.3	1.1	802	16
FC1-7	A	8_7	325	1807	0.3	23.0	1.4	820	17
FC1-7	A	8_8	326	965	1.1	43.0	2.6	888	19
FC1-7	A	9_2	327	5223	2.5	8.0	0.6	721	17
FC1-7	A	9_3	328	2613	0.4	15.9	0.9	783	16
FC1-7	A	9_4	329	2013	0.5	20.6	1.2	809	17
FC1-7	A	9_5	330	1879	0.2	22.1	1.3	816	17
FC1-7	A	9_6	331	2124	0.9	19.6	1.2	804	17
FC1-7	A	9_7	332	2001	0.5	20.8	1.2	809	17
FC1-7	A	9_8	333	1696	0.7	24.5	1.5	826	17
FC1-7	A	9_9	334	441	3.9	94.1	7.1	986	26
FC1-7	A	10_2	335	5132	5.3	8.1	1.0	723	25
FC1-7	A	10_3	336	2984	1.8	13.9	0.9	771	17
FC1-7	A	10_4	337	2208	0.8	18.8	1.1	800	17
FC1-7	A	10_5	338	1899	0.5	21.9	1.3	815	17
FC1-7	A	10_6	339	1963	0.2	21.2	1.2	811	17
FC1-7	A	10_7	340	2065	0.5	20.1	1.2	806	17
FC1-7	A	10_8	341	1833	1.0	22.7	1.4	818	17
FC1-7	A	10_9	342	1614	1.0	25.7	1.6	831	18
FC1-7	A	11_3	343	3750	1.9	11.1	0.8	750	17
FC1-7	A	11_4	344	2328	0.6	17.8	1.1	795	16
FC1-7	A	11_5	345	1979	0.6	21.0	1.3	811	17
FC1-7	A	11_6	346	1805	0.7	23.0	1.4	820	17
FC1-7	A	11_7	347	1930	0.7	21.5	1.3	813	17
FC1-7	A	11_8	348	2003	0.7	20.7	1.2	809	17
FC1-7	A	11_9	349	1756	0.9	23.6	1.4	823	17
FC1-7	A	11_10	350	342	9.9	121.5	14.2	1021	41
FC1-7	A	12_3	351	2809	4.6	14.8	1.5	777	24
FC1-7	A	12_4	352	2315	1.0	17.9	1.1	795	17
FC1-7	A	12_5	353	2090	1.0	19.9	1.2	805	17
FC1-7	A	12_6	354	1859	0.3	22.3	1.3	817	17
FC1-7	A	12_7	355	1820	0.3	22.8	1.3	819	17
FC1-7	A	12_8	356	1862	0.6	22.3	1.3	817	17
FC1-7	A	12_9	357	1864	0.8	22.3	1.3	817	17
FC1-7	A	12_10	358	1098	4.0	37.8	3.4	873	25
FC1-7	A	12_11	359	198	16.8	209.3	17.7	1104	35
FC1-7	A	13_4	360	2678	1.0	15.5	1.0	781	16
FC1-7	A	13_5	361	2175	0.6	19.1	1.1	801	16
FC1-7	A	13_6	362	2062	0.7	20.1	1.2	806	17

FC1-7	A	13_7	363	1840	0.3	22.6	1.3	818	17
FC1-7	A	13_8	364	1736	0.5	23.9	1.4	824	17
FC1-7	A	13_9	365	1676	0.7	24.8	1.5	827	17
FC1-7	A	13_10	366	1694	0.5	24.5	1.5	826	17
FC1-7	A	13_11	367	796	27.9	52.2	23.5	910	125
FC1-7	B	1_3	368	4008	6.0	10.4	1.3	744	28
FC1-7	B	1_4	369	2043	1.6	20.3	1.3	807	18
FC1-7	B	1_5	370	2262	0.5	18.4	1.1	797	16
FC1-7	B	1_6	371	2105	0.8	19.7	1.2	804	17
FC1-7	B	1_7	372	1635	0.6	25.4	1.5	830	17
FC1-7	B	1_8	373	1511	0.2	27.5	1.6	838	17
FC1-7	B	1_9	374	1479	0.6	28.1	1.7	841	18
FC1-7	B	1_10	375	343	1.6	121.1	7.4	1021	24
FC1-7	B	2_4	376	3512	3.1	11.8	1.0	756	20
FC1-7	B	2_5	377	2202	0.9	18.9	1.2	800	17
FC1-7	B	2_6	378	2393	0.5	17.4	1.0	792	16
FC1-7	B	2_7	379	2078	1.3	20.0	1.3	806	17
FC1-7	B	2_8	380	1544	0.4	26.9	1.6	836	17
FC1-7	B	2_9	381	1438	0.7	28.9	1.7	844	18
FC1-7	B	2_10	382	1417	0.7	29.3	1.8	845	18
FC1-7	B	2_11	383	992	5.0	41.8	4.3	885	29
FC1-7	B	3_5	384	2193	3.0	18.9	1.5	800	21
FC1-7	B	3_6	385	2449	0.6	17.0	1.0	790	16
FC1-7	B	3_7	386	2759	0.7	15.1	0.9	778	16
FC1-7	B	3_8	387	2046	0.5	20.3	1.2	807	17
FC1-7	B	3_9	388	1514	1.1	27.4	1.7	838	18
FC1-7	B	3_10	389	1370	0.6	30.3	1.8	849	18
FC1-7	B	3_11	390	819	4.1	50.7	4.5	907	27
FC1-7	B	3_12	391	173	5.3	240.7	14.6	1127	27
FC1-7	B	4_6	392	2341	1.0	17.7	1.1	794	17
FC1-7	B	4_7	393	2382	1.2	17.4	1.1	792	17
FC1-7	B	4_8	394	2431	0.7	17.1	1.0	790	16
FC1-7	B	4_9	395	1896	0.3	21.9	1.3	815	17
FC1-7	B	4_10	396	1489	0.8	27.9	1.7	840	18
FC1-7	B	4_11	397	1432	0.5	29.0	1.7	844	18
FC1-7	B	4_12	398	786	34.3	52.8	29.8	912	156
FC1-7	B	5_7	399	1628	8.5	25.5	4.3	831	41
FC1-7	B	5_8	400	2342	0.3	17.7	1.0	794	16
FC1-7	B	5_9	401	2391	0.9	17.4	1.1	792	16
FC1-7	B	5_10	402	1824	0.2	22.8	1.3	819	17
FC1-7	B	5_11	403	1316	0.4	31.5	1.9	853	18
FC1-7	B	5_12	404	1286	0.3	32.3	1.9	856	18
FC1-7	B	5_13	405	360	0.9	115.5	6.9	1014	23
FC1-7	B	6_8	406	2432	1.8	17.1	1.2	790	18
FC1-7	B	6_9	407	2272	0.6	18.3	1.1	797	16
FC1-7	B	6_10	408	2211	0.6	18.8	1.1	800	16

FC1-7	B	6_11	409	1668	1.0	24.9	1.5	828	18
FC1-7	B	6_12	410	1342	1.0	30.9	1.9	851	18
FC1-7	B	6_13	411	372	1.9	111.5	7.0	1009	24
FC1-7	B	7_8	412	1867	1.9	22.2	1.5	816	19
FC1-7	B	7_9	413	2148	0.8	19.3	1.2	802	17
FC1-7	B	7_10	414	2048	1.0	20.3	1.2	807	17
FC1-7	B	7_11	415	1992	0.3	20.9	1.2	810	17
FC1-7	B	7_12	416	1152	1.2	36.0	2.2	868	19
FC1-7	B	7_13	417	237	1.6	175.0	10.5	1076	25
FC1-7	B	8_9	418	2347	1.6	17.7	1.2	794	17
FC1-7	B	8_10	419	1967	0.7	21.1	1.3	811	17
FC1-7	B	8_11	420	1886	0.7	22.0	1.3	815	17
FC1-7	B	8_12	421	1659	0.4	25.0	1.5	829	17
FC1-7	B	8_13	422	301	2.1	138.1	8.7	1040	25
FC1-7	B	9_10	423	2267	1.2	18.3	1.2	797	17
FC1-7	B	9_11	424	1848	1.4	22.5	1.4	817	18
FC1-7	B	9_12	425	1600	1.7	26.0	1.7	832	19
FC1-7	B	9_13	426	1076	3.1	38.6	3.1	875	23
FC1-7	B	10_11	427	1724	4.7	24.1	2.5	825	27
FC1-7	B	10_12	428	601	1.3	69.1	4.3	945	21
FC1-7	B	1_3	429	3080	0.8	13.5	0.8	768	16
FC1-7	B	1_4	430	2070	0.2	20.1	1.2	806	16
FC1-7	B	1_5	431	2095	0.9	19.8	1.2	805	17
FC1-7	B	1_6	432	1820	0.7	22.8	1.4	819	17
FC1-7	B	1_7	433	1493	0.3	27.8	1.6	840	17
FC1-7	B	1_8	434	1415	0.6	29.3	1.7	845	18
FC1-7	B	1_9	435	1427	0.5	29.1	1.7	844	18
FC1-7	B	1_10	436	196	19.3	211.6	32.1	1106	59